# LAMINAR AND HEAT TRANSFER IN HELICAL COILS

BY

SALAH AL-DEEN BUORHAN AL-OMARI

SUPERVISOR

Dr. NASRI J. RABADI

Submitted in partial fulfillment of the requirements for the degree of master of science in mechanical engineering.

Faculty of Graduate Studies,

University of Jordan.

Amman , Jordan

April , 1991

# ACKNOWLEDGEMENT

I wish to express my gratitude to every body who contributed in the completion of this work. Special feeling of gratitude to my advisor Dr. N. Rabadi for his assistance and guidance. Also I express my thanks to my friends Hazim Ali and Mohammed Haijawi for their assistance.

My grateful acknowledgment is extended to all members of my family for their love and encouragement.

# Abstract

Laminar viscous flow and heat transfer in helical coils are studied numerically. The effect of coil pitch on fluid flow and heat transfer is described. It is assumed that coil radius is much greater than that of the tube. The thermal boundary condition considered is constant wall temperature. Prandtl number range considered is from 0.05 to 40, and Dean number range is from 60 to 328. Coil curvature ratio studied is 100. The numerical method used to solve for flow and thermal fields is the alternating direction implicit method (ADI). Good stability in the numerical solution is noticed when a convergence parameter is introduced into the ADI method. It is concluded that coil pitch angles up to 30° have negligible effect on convective heat transfer. However, pitch angles up to 45° are found to decrease the average Nusselt number by about 20% in the case of intermediate and high Prandtl number. The reduction is about 10% in the case of low Prandtl number.

# Contents

# NOMENCLATURE

| | |
|---|---|
| $a$ | Tube radius |
| $De$ | Dean number ( $= Re/R^{1/2}$ ) |
| $Nu$ | Local Nusselt number |
| $\overline{Nu}$ | Peripherally averaged Nusselt number |
| $Pr$ | Prandtl number |
| $r$ | Dimensionless tube radius ( $= r'/a$ ) |
| $R$ | Dimensionless coil radius ( $= R'/a$ ) |
| $Re$ | Renolds number ( $Re = 2aw/\nu$ ) |
| $T$ | Dimensionless tem p erature |

$$T = [(T_w - T)/ \ (Pr\ \partial T/\partial\theta)]\ [(T_w - T_m)/(T_w - T_c)]$$

| | |
|---|---|
| $T_c$ | Dimensionless temperature at the center-line of the tube |
| $T_w$ | Dimensionless temperature at the wall |
| $T_m$ | Dimensionless mixing cup temperature |
| $u$ | Dimensionless radial component of velocity ( $= u'a/\nu$ ) |
| $v$ | Dimensionless tangential component of velocity ( $= v'a/\nu$ ) |
| $w$ | Dimensionless axial component of velocity ( $= w'a/\nu$ ) |

Greek symbols

| | |
|---|---|
| $\alpha$ | Pitch angle |
| $\phi$ | Angular coordinate in tube cross-section |
| $\theta$ | Angular coordinate in plane of tube curvature |
| $\lambda$ | Convergence parameter |
| $\nu$ | Fluid kinematic viscosity |

Superscripts

| | |
|---|---|
| ' | Denotes dimensional quantities |

# LIST OF TABLES

# LIST OF FIGURES

# CHAPTER 1

## INTRODUCTION

The study of flow and heat transfer in curved tubes is a research problem of great practical interest. Applications of such flows are found in many important flow and heat transfer applications. For example thermal storage tanks, rocket engines, jacketed vessels, reacting vessels and heating, ventilating and air conditioning systems.

One important feature of the flow in curved tubes is the secondary flow. Understanding the physical phenomenon of the secondary flow in curved tubes is very important since it is the mechanism that makes such flows unique and interesting. Centrifugal force, proportional to the square of the axial velocity, tends to push fluid in the central region of the tube cross section towards the outer bend of the curved tube. This induces a pressure gradient directed towards the inner bend of the tube, with a maximum pressure at the outer bend. As a result of the variation of the axial velocity throughout the tube cross-section, the centrifugal force assumes its greatest magnitude in the central region and is roughly in balance with the induced pressure gradient (Prusa and Yao, 1982).

The pressure near the wall decreases circumferentially going from the outer side to the inner side of the tube cross-section. The fluid close to the wall will move from higher pressure regions to lower pressure regions. Hence, secondary motion will be induced in both halves of the tube cross-section.

The axial velocity profile along the horizontal diameter, i.e. diameter of symmetry, is distorted from the familiar parabolic profile encountered in flows in horizontal straight tubes. Although the maximum axial velocity, still lies on the horizontal diameter, it is shifted to the outer side of the tube cross section. This is due to the centrifugal force acting on fluid particles.

One consequence of secondary flow inside curved tubes is increasing the critical Reynolds number. The secondary flow circulates the high kinetic energy fluid from the central core of the tube towards the wall region where the fluid flows slower. The mixing which results delays the flow transition to turbulent flow.

Fully developed laminar curved tube flows are characterized by the ratio of centrifugal forces to viscous forces. This ratio is known as the Dean number, $De=Re/R^{1/2}$ where Re is the Reynolds number and R is the curvature ratio $R'/a$ , where $R'$ is the coil radius, and a is the tube radius.

Heat transfer rate in curved tubes is proved to be significantly greater than in straight tubes under the same boundary conditions and for the same mass flow rate. This is due to the mixing effect caused by secondary motion.

The most important thermal boundary conditions that have been considered for heat transfer in curved tubes are axially uniform wall heat flux with uniform wall temperature at each axial location, and constant wall temperature.

The objective of this study is to investigate the fully developed laminar flow and heat transfer in helically coiled tubes. The coil radius is taken to be very high in comparison with tube radius, i.e. $R' \gg a$. The thermal boundary condition considered is constant wall temperature. The effect of different inclination angles of the tube axis, i.e. different coil pitch angles, on both flow and heat transfer is presented. Results are given for the range of Dean number from 60.0 to 328.0, curvature ratio of 100 , and Prandtl number of0.05, 1.0, 5.0, 25.0,and 40.0 . For fluid flow , results are given in the form of secondary flow contours, and axial velocity distribution along the horizontal diameter of the tube cross-section. For heat transfer, results are presented in the form of temperature contours, local Nusselt number, and average Nusselt number.

# CHAPTER 2

## LITERATURE REVIEW

Fully developed flow and heat transfer in curved tubes was studied extensively by many researchers both theoretically and experimentally for different thermal boundary conditions. However, the effect of coil pitch has not been studied adequately.

The first theoretical study of fully developed steady flow in a curved tube with circular cross section was made by Dean ( 1927 ). He pointed out that the dynamic similarity of such flow depends on a non - dimensional parameter $k = (2a/R')(aW_m/\nu)$ , where $W_m$ is the mean axial velocity , $\nu$ is the kinematic viscosity and a is the radius of the pipe which is bent in a circle with a radius $R'$. This parameter can be considered as the ratio of the centrifugal force induced by circular motion of the fluid to the viscous force. Dean's analysis was restricted to small values of k.

White ( 1929 ) presents extensive experimental data for helical flow. His data have been correlated by a dimensionless quantity, known now as Deans number, which is equal to the Reynolds number multiplied by the square root of the ratio between the tube radius to the coil radius.

Haves ( 1932 ) presents experimental data of axial velocity in curved tubes and shows their distortion from parabolic profiles characteristic of horizontal straight tubes, due to the induced centrifugal forces by circular motion. He shows that the temperature profiles are different from those for straight tubes and that the local heat transfer coefficient at the outer wall is greater than that at the inner wall. He is the first to present the fully developed temperature profiles in curved tubes experimentally.

Adler ( 1934 ) experimentally verifies the hydrodynamic results obtained by Hawes for curvature ratios $R'/a$ 50, 100, and 200.

Truesdell and Adler ( 1970 ) treat laminar flow in helically coiled tubes numerically. Fully developed axial and secondary velocities are calculated for both circular and elliptical cross sections. Only coils with small pitch angles are considered.

Murakami et. al. ( 1971 ) report that the effect of non-zero pitch could be approximately accounted for by using modified radius of curvature in the Dean number calculation as follows :

$$De = Re \left( \frac{a}{\rho} \right)^{1/2}$$

where

$$\rho = R' ( 1 + \tan^2\alpha )$$

where $\rho$ is the modified radius of curvature, and $\alpha$ is the pitch angle.

Austin ( 1971 ) numerically solves for flows inside circular coils with Dean number ranging from 1 to 1000 and with curvature ratio from 5 to 100. The flow equations solved were put in terms of axial velocity, stream function, and vorticity. Although considerable computation time was needed, his results agree well with accepted experimental data.

Dravid, Smith, Merril and Brian ( 1971 ) present experimental, analytical and numerical results for laminar flow in helically coiled tubes with small pitch with an emphasis on a fundamental understanding of developing temperature field. The differential equation of heat transport is solved in two steps : First, an analytical approximation applicable within about one tube radius from the start of the heat transfer zone, and second, the complete numerical solution covering both the entire thermal entrance region and the fully developed region. Numerical results are compared with experimental data in the range in which they overlap. Three wall boundary conditions are considered, 1) constant wall temperature. 2) constant wall heat flux. and 3) wall heat flux varies with angular direction $\phi$ so that the temperature is independent of $\phi$ at any axial location.

Kalb and Seader ( 1971 ) treat steady viscous flow in curved circular tubes for fully developed velocity and temperature fields under the thermal boundary condition of axially uniform wall heat flux with peripherally uniform wall temperature. The thermal energy equation was solved numerically by the use of a point successive over relaxation method. Results cover a wide range of Dean number, Prandtl number and curvature ratio. The Dean number ranges from 1 to 1200, Prandtl number from 0.005 to 1600 and curvature ratio from 10 to 100. Peripherally averaged Nusselt number is correlated by the following equations :

$$\overline{Nu} = 3.31 \ De^{0.115} \ Pr^{0.0108} \qquad 20 < De < 1200, \quad 0.005 < Pr < 0.05$$

with a maximum deviation of 4 % .

$$\overline{Nu} = 0.913 \ De^{0.476} \ Pr^{0.2} \qquad 80 < De < 200, \quad 0.7 < Pr < 5.0$$

with a maximum deviation of 5 %.

Kalb and Seader ( 1974 ) consider flow and heat transfer in curved circular tubes for a uniform wall temperature boundary condition. They give numerical solutions for a wide range of Prandtl numbers for Dean numbers as high as 1200. For values as small as 10, the curvature ratio is found to have a negligible effect on the peripherally averaged Nusselt number. The average Nusselt numbers for the important Prandtl number range of 0.7 to 5 are correlated by

$$\overline{Nu} = 0.836 \ De^{0.5} \ Pr^{0.1} \qquad De > 80$$

Janssen and Hoogendoorn ( 1978 ) present an experimental and numerical study on convective heat transfer in coiled tubes. They consider heat transfer in the thermal entry region as well as in fully developed thermal and hydrodynamic regions. Two thermal boundary conditions were studied; uniform peripherally averaged heat flux, and constant wall temperature. The experiments were carried out for curvature ratios, R , from 100 to 10, Prandtl numbers from 10 to 500 and Reynolds number from 20 to 4000.

Rabadi, Chow, and Simon ( 1979 ) solve the flow and heat transfer equations numerically, using a modified procedure that covers a wide range of Prandtl numbers and Dean numbers up to 1305. The thermal boundary condition analyzed is axially uniform wall heat flux and peripherally uniform wall temperature. It is found that the secondary flow circulations become more complex as the Dean number increases. A convergence parameter is introduced into the alternating direction implicit ( ADI ) method, which results in a substantially reduced computation time. A method of finding the optimum convergence parameter is described. Their results are compared for the same range of parameters with those of Austin ( 1971 ).

Zapryanov, Christov and Toshev ( 1979 ) present a numerical study of fully developed steady flow of viscous incompressible fluid in a curved circular tube. The numerical solution applies the method of fractional steps to hydrodynamic and thermal problems. Good solutions from low to reasonably high Dean and Prandtl numbers are obtained. Results are compared with experimental data and some theoretical solutions.

Chilukuri and Humphrey ( 1980 ) study the influence of buoyant effects on developping heat transfer in strong curved duct flows. They assume steady state, incompressible laminar flow of constant physical property fluid.

Prusa and Yao ( 1982 ) introduce a physical model that accounts for the combined effects of both buoyancy and centrifugal force for fully developed laminar flow in heated curved tubes. A thermal boundary condition so that a constant axial temperature gradient is maintained is used. Results for Prandtl number of unity are presented for a moderate range of Dean number and product of the Reynolds and Raleigh numbers. Detailed predictions of flow resistance, average heat transfer rate and secondary flow streamlines are given. A flow-regime map is provided to indicate the three basic regions where ( 1 ) centrifugal force dominates ( 2 ) both buoyancy and centrifugal forces are important and ( 3 ) buoyancy force dominates.

Kalb and Seader ( 1982 ) present experimental study of entrance region heat transfer to gases flowing in a uniform wall temperature helical coil. Runs were made in the range of Reynolds number where the flow is initially turbulent upon entering the coil, but laminar downstream where secondary flow develops. The results indicate a rapid transition to laminar flow and are in satisfactory agreement with a numerical solution for fully developed heat transfer.

Humphrey, Iacovides and Launder ( 1985 ) give numerical solutions for a semi-truncated Navier-Stokes equations for the case of developing laminar flow in circular-sectioned bends over a range of Dean numbers. The ratios of bend radius to pipe radius are 7:1 and 20:1. Stream wise velocity profiles at Dean numbers of 183 and 565 are in excellent agreement with Laser-Doppler measurements by Agrawal, Talbot and Gong ( 1978 ).

Futagami and Aoyama ( 1988 ) present both theoretical and experimental study on the effect of secondary flow on heat transfer from a uniformly heated helically coiled tube to fully developed laminar flow. Both the centrifugal and buoyancy forces are taken into account in the numerical analyses. The solutions cover a wide range of Prandtl numbers. The velocity and temperature profiles, the friction factor and heat transfer coefficient are obtained. The effects of the secondary flow on heat transfer are divided into three types; those in the centrifugal, the buoyant and the composite range. They give an approximate expression for peripherally averaged Nusselt number in the composite range. Their results are compared with experimental results using water. The coil used in the experiments have a curvature ratio of 101:1 and the angle of inclination of the coil axis is 7°.

Sumida, Suodou, and Wada ( 1989 ) clarify experimentally the secondary flow pattern by visulization method for fully developed pulsating flow through curved pipe with curvature ratio of 7.6.

Rabadi (1989 ) uses the Alternating Direction Implicit method ( ADI ) to solve the energy equation for viscous flow in coils. The thermal boundary condition considered is constant wall temperature. A convergence parameter is introduced into the ADI method resulting in a substantially reduced computation time and high flexibility of solution. Temperature contours for Dean number of 594 over a range of Prandtl number from 0.05 to 5 are presented, and also for

De=1390 and Pr =5.0. Results for both local and average Nusselt number are given for the above mentioned values of both Dean number and Prandtl number. Average Nusselt number was correlated by the following formula for Prandtl number of 0.7, and 5.0

$$\overline{Nu} = 0.507\ De^{.611} Pr^{0.116} \qquad 100 \le De \le 1300$$

$$0.7 \le Pr \le 5.0$$

# CHAPTER 3

# FORMULATION OF THE PROBLEM

## 3.1 Assumptions

In this study the following assumptions are made :

1) Incompressible, Newtonian, and constant properties fluid.
2) Steady laminar flow.
3) The flow and temperature fields are fully developed.
4) Negligible free convection and viscous dissipation.
5) Negligible axial conduction relative to radial conduction.
6) The tube radius is very small in comparison with the coil radius, that is $a/R' \ll 1$

## 3.2 Governing equations for helical coils

The dimensional equations that govern steady laminar flow and heat transfer in helical coils ( figure 3-1 ) are given as follows ( Futagami and Aoyama, 1987 ) :

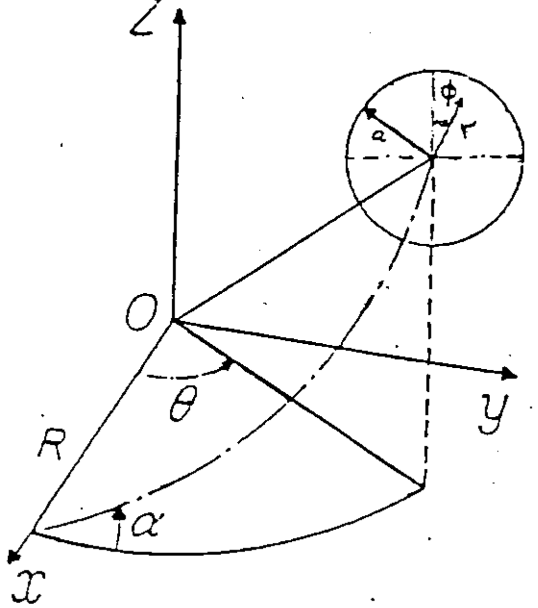


Figure 3.1 : System of helical coordinates

Continuity equation :

$$\frac{\partial u}{\partial r} + \frac{1}{r}\frac{\partial v}{\partial \phi} + \frac{u}{r} = 0 \qquad (3.1)$$

Momentum equations :

Radial-direction motion

$$u\frac{\partial u}{\partial r} + \frac{v}{r}\frac{\partial u}{\partial \phi} - \frac{v^2}{r} - \frac{\cos^2\alpha \cos\phi}{R} w^2$$

$$= -\frac{1}{\rho}\frac{\partial P}{\partial r} + \nu\left[\Delta u - \frac{u}{r^2} - \frac{2}{r^2}\frac{\partial v}{\partial \phi}\right] \qquad (3.2)$$

Tangential-direction motion

$$u\frac{\partial v}{\partial r} + \frac{v}{r}\frac{\partial v}{\partial \phi} + \frac{uv}{r} \frac{\cos^2\alpha \sin\phi}{R} w^2$$

$$= -\frac{1}{\rho}\frac{\partial P}{\partial \phi} + \nu\left[\Delta u - \frac{v}{r^2} + \frac{2}{r^2}\frac{\partial u}{\partial \phi}\right] \qquad (3.3)$$

Axial-direction motion

$$u\frac{\partial w}{\partial r} + \frac{v}{r}\frac{\partial w}{\partial \phi} = -\frac{\cos\alpha}{\rho R}\frac{\partial P}{\partial \theta} + \nu\Delta w \qquad (3.4)$$

where $v'$, $u'$ and $w'$ are the dimensional velocity components in the tangential, radial and axial directions respectively.

Energy equation

$$u \frac{\partial T}{\partial r} + \frac{v}{r} \frac{\partial T}{\partial \phi} + \frac{w}{R} \frac{\partial T}{\partial \theta} = \varkappa \, \Delta T \qquad (3.5)$$

here $T'$, $p'$, and $\varkappa$ are the dimensional temperature, pressure, and thermal diffusivity respectively.

The operator $\Delta$ is given as follows:

$$\Delta = \frac{\partial^2}{\partial r^2} + \frac{1}{r} \frac{\partial}{\partial r} + \frac{1}{r^2} \frac{\partial^2}{\partial \phi^2}$$

The above system of equations can be put in a simpler form by eliminating the un-known pressure gradients in both r and $\phi$ directions from equations (3-2) and (3-3). This can be achieved by differentiating equation (3-2) with respect to $\phi$ and equation (3-3) with respect to $r'$, and then combining the resulting two equations so that the un-known pressure terms are canceled. This results in a new equation named secondary flow equation, since it represents secondary flow. But still the resulted equation has a complex form and need to be simplified more. This is achieved by introducing both the radial and tangential velocity components ( $u'$ and $v'$ ) in terms of the dimensional stream function $\psi'$ as follows:

$$u = -\frac{1}{r}\frac{\partial\psi}{\partial\phi} \qquad (3.6)$$

$$v = \frac{\partial\psi}{\partial r} \qquad (3.7)$$

When both u' and v' are used in their new forms as given by equations ( 3-6 ) and ( 3-7 ), the equation resulted earlier from the differentiating and combining process mentioned above ( refer ed to as secondary flow equation ) is transformed into a fourth order equation in terms of $\psi$. And so the final set of equations governing the flow field is composed of two simultaneous partial differential equations; the first is second order ( in terms of w ) represents axial flow, and the second is fourth order ( in terms of $\psi$ ) represents secondary flow.

The fourth order secondary flow equation can be further simplified using the following definition of axial vorticity $\xi'$. The resulted new secondary flow equation is second order in terms of $\xi$, where $\xi$ is given as follows :

$$\xi' = \Delta\psi' \qquad (3.8)$$

The dimensional form of the secondary flow equation is given as follows:

$$u\frac{\partial\xi}{\partial r} + \frac{v}{r}\frac{\partial\xi}{\partial\phi} =$$

$$\frac{2\ v\ \cos^2\alpha}{R}\left[\sin\phi\ \frac{\partial w}{\partial r} - \frac{1}{r}\cos\phi\frac{\partial w}{\partial\phi}\right] + \nu\Delta\xi \qquad (3.9)$$

Non-dimensionalizing the governing equations:

The flow field equations can be made dimensionless using the following transformations :

$$w = \frac{aw}{\nu} \quad , u = \frac{au}{\nu} \quad , v = \frac{av}{\nu} \qquad r = \frac{r}{a} \quad , R = \frac{R}{a}$$

$$\psi = \frac{\psi}{\nu} \quad , \xi = \frac{a^2\xi}{\nu} \quad , P = \frac{a^2 P}{\rho \ \nu 2}$$

The resulting dimensionless equations that govern flow and temperature fields are given below :

Dimensionless axial velocity equation :

$$u \frac{\partial w}{\partial r} + \frac{v}{r} \frac{\partial w}{\partial \phi} = - \frac{\cos \alpha}{R} \frac{\partial P}{\partial \theta} + \Delta w \qquad (3.10)$$

The operator $\Delta$ is as follows :

$$\Delta = \frac{\partial^2}{\partial r^2} + \frac{1}{r} \frac{\partial}{\partial r} + \frac{1}{r^2} \frac{\partial^2}{\partial \phi^2}$$

Using both u and v in their form as functions of $\psi$ ( $u = (-1/r)\ (\partial\psi/\partial\phi)$ , $v = \partial\psi/\partial r$ ) Equation ( 3-10 ) becomes :

$$C \frac{\partial w}{\partial r} + B \frac{\partial w}{\partial \phi} - \frac{\partial^2 w}{\partial r^2} - \frac{1}{r^2} \frac{\partial^2 w}{\partial \phi^2} = - \frac{\cos \alpha}{R} \frac{\partial P}{\partial \theta} \qquad (3.11)$$

where :

$$B = \frac{1}{r} \frac{\partial \psi}{\partial r} \quad , \quad C = - \frac{1}{r} - \frac{1}{r} \frac{\partial \psi}{\partial \phi}$$

Dimensionless secondary flow equation :

$$C \frac{\partial \xi}{\partial r} + B \frac{\partial \xi}{\partial \phi} - \frac{\partial^2 \xi}{\partial r^2} - \frac{1}{r^2} \frac{\partial^2 \xi}{\partial \phi^2} = D_v \qquad (3.12)$$

where

$$D_v = \frac{2\, w \cos^2\alpha}{R} \left[ \cos\phi \frac{\partial w}{\partial r} - \frac{1}{r} \sin\phi \frac{\partial w}{\partial \phi} \right]$$

$$\xi = \Delta\psi$$

Dimensionless energy equation :

To make the energy equation dimensionless, all previously mentioned dimensionless quantities are to be used in addition to the following dimensionless temperature for the thermal boundary condition of constant wall temperature :

$$T = \frac{T_v - T}{Pr\ \partial T_m / \partial \theta} \qquad \frac{T_v - T_m}{T_v - T_c}$$

where Pr is the Prandtl number ( $Pr = \mu c_p / k$ ), $T_v$ is the wall temperature, $T_m$ is the mixing-cup temperature, and $T_c$ is the temperature at the center-line of the tube.

The resulting dimensionless energy equation is given as :

$$Pr \left( u \frac{\partial T}{\partial r} + \frac{v}{r} \frac{\partial T}{\partial \phi} \right) + \frac{w}{R} \frac{T}{T_c} = \Delta T \qquad (3.13)$$

where the operator $\Delta$ is as defined in page 20

## 3.3 Boundary conditions

The boundary conditions of the governing equations are shown in figure ( 3-2 ). A discussion of those boundary conditions is given below :

### 3.3.1 Axial velocity boundary conditions

1) At the wall ; The no-slip condition applies, hence $w_{r=1} = 0$.

2) Along the horizontal diameter ; Derivative boundary conditions are present, due to symmetry between the upper and lower halves of the tube cross-section; $(\partial w/\partial \phi)_{\phi=\pm\pi/2} = 0$ .

3) At the center point of the tube-cross section; A derivative boundary condition is present. This is because of symmetry along the vertical diameter at the center point, $(\partial w/\partial r)_{r=0} = 0$

### 3.3.2 Stream function boundary conditions

1) At the wall; The wall represents a streamline along which $\psi$ has a constant value. For convenience this constant value is taken to be zero since there is no significance for the absolute value of $\psi$. Only derivatives of $\psi$ are meaningful.

2) Along the horizontal diameter; What is said in item 1 is applicable here, since the horizontal diameter represents a streamline. Because of its continuous nature a value of zero is assigned to $\psi$ .

3) At the center point of the tube-cross section; Because of the continuous nature of the stream function, it must have the value of zero at the center point.

### 3.3.3 Vorticity boundary conditions

Equation ( 3-8 ) will be used to illustrate the vorticity boundary conditions :

1) At the wall; Because of the no-slip condition at the wall Equation 3-8 gives :

$$\xi_{r=1} = \left(\frac{\partial^2 \psi}{\partial r^2}\right)_{r=1}$$

2) Along the horizontal diameter; Equation 3-8 gives $\xi = 0$

3) At the center point of the tube cross section; Since the axial vorticity is a continuous function it must have a

zero value at the center point.

### 3.3.4 TEMPERATURE BOUNDARY CONDITIONS

1) At the wall; From the definition of T, it is obvious that T is zero at the wall.
2) Along the horizontal diameter; Because of symmetry, the derivative boundary condition of $(\partial T/\partial \phi)_{=\pi/2} = 0$ holds.

3) At the center point of the tube-cross section; At the center point symmetry along the vertical diameter rquires

$$(\partial T/\partial r)_{r=0} = 0$$

## 3.4 Dean number and Nusselt number calculation

The Dean number is evaluated from the following relation:

$$De = Re\ (\ a/R\ )^{1/2}$$

The Local Nusselt number is derived from the following relation:

$$q_w = -\ k\ (\partial T/\partial r)_{r=a} = h\ (\ T_w - T_m)$$

where $q_w$ is the heat flux at the wall, and $T_m$ is the mean temperature. After making the above relation dimensionless, using the previously defined transformations, local Nusselt number can be shown to be given as follows:

$$Nu = \frac{-2\ (\ \partial T/\partial r)_{r=1}}{T_m}$$

$T_m$ is defined by:

$$T_m = \frac{1}{W_m \pi} \int_0^{2\pi} \int_0^{1} W\ T\ r\ dr\ d\phi$$

Average nusselt number is given by :

$$\overline{Nu} = -\ \frac{1}{\pi\ R\ T_m} \int_0^{2\pi} (\partial T/\partial r)_{r=1} R\ d\phi$$

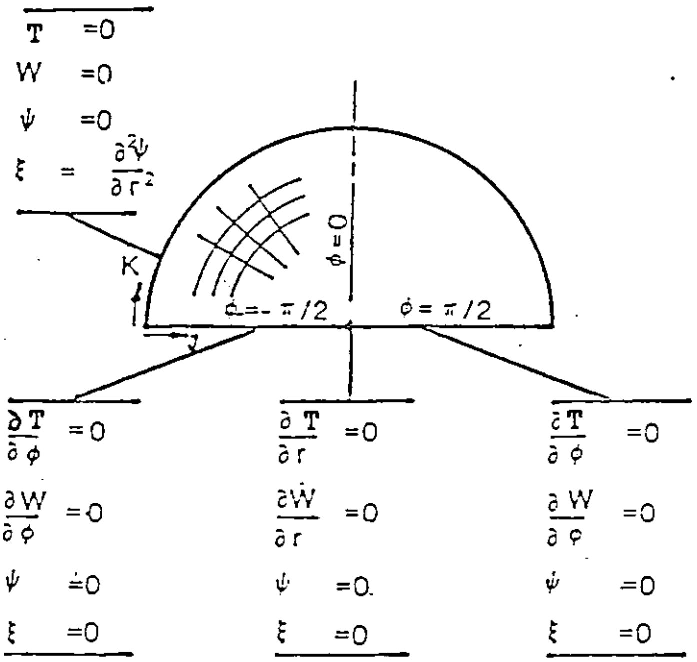


Figure 3.2 Boundary conditions

# CHAPTER 4

# NUMERICAL SOLUTION

## 4.1 Introduction

Before going into the details of the numerical solution, the following remarks are to be mentioned :

1) The axial velocity, secondary flow, and energy equations are all non-linear and although mathematically being classified elliptic, they can be considered, approximately, parabolic. This is because in such fluid flow problems, influences travel only from upstream to downstream, i.e. the conditions at a point are affected largely by the upstream conditions, and very little by downstream ones. On the other hand equation 3-8, that gives the definition of vorticity is linear and elliptic.

2) The governing flow equations are linked with each other, and are to be solved simultaneously, where as can be seen, the secondary flow equation has axial velocity terms, and so can not be solved unless the axial velocity field is known; either from initial guess or from the solution of axial flow equation. The stream function $\psi$ is obtained from Equation 3-8 after each iteration cycle. This equation depends on $\xi$ values, which are obtained either from initial guess, or from the solution of the secondary flow equation, Eq. 3-12 . The axial velocity equation is linked with both

secondary flow equation and the vorticity equation through the non-linear coefficients which are functions of $\psi$.

3) After getting the flow field solution, the energy equation can be solved, where the energy equation is linked with velocity field through the presence of convectional terms and source term.

## 4.2 Numerical methods used

Alternating Direction Implicit ( ADI ) methods were introduced in companion papers by Peacemen and Rachford (1955) and Douglas ( 1955 ). ADI method proposed by Peacemen and Rachford make use of splitting time step ( in case of un-steady problems) or iteration step ( in case of steady state problems) into two halves for two-dimensional problems, three halves for three-dimensional problems, and so on. It was used successfully (Rabadi, 1980) by wilkes ( 1963 ), Pearson ( 1965,1967 ), Brily ( 1968 ) and Rabadi et. al. ( 1979 ). ADI methods are currently the most popular approach to viscous flow problems . Because of these reasons, the ADI method proposed by Peacemen and Rachford ( 1955 ) is used in this study to solve axial flow, secondary flow and energy equations.

For elliptic equations, the successive over-relaxation (SOR) method was used effectively in previous works (Rabadi, 1980), and hence it is used in this study to obtain new field values of $\psi$ when solving equation 3-8 at the end of each iteration cycle.

The SOR method can be summarized using the following equation; where it describes how new values of $\psi$ at the end of the iteration step can be evaluated :

$$\psi^{i+1} = \beta\, E + \psi^{i}(\, 1-\beta\,)$$

where; $\beta$ is an over relaxation parameter; $1 < \beta < 2$ .

E is the value of $\psi$ obtained from the solution of vorticity equation ( Eq. 3-8 ).

## 4.3 Finite difference equations

The finite-difference form of the governing equations, according to ADI method, is given below, where central differences are used :

The finite difference equation of the first half of the iteration step is given by :

$$X_1^{i}\, Y_{j-1,k}^{i+1/2} + X_3^{i}\, Y_{j,k}^{i+1/2} + X_5^{i}\, Y_{j+1,k}^{i+1/2} =$$

$$Q - X_2^{i}\, Y_{j,k-1}^{i} - X_6^{i}\, Y_{j,k}^{i} - X_4^{i}\, Y_{j,k+1}^{i} \qquad (4.1)$$

The finite difference equation of the second half of the iteration step is given by :

$$X_2^i \, Y_{j,k-1}^{i+1} + X_6^i \, Y_{j,k}^{i+1} + X_4^i \, Y_{j,k+1}^{i+1} =$$

$$Q - X_1^i \, Y_{j-1,k}^{i+1/2} - X_3^i \, Y_{j,k}^{i+1/2} - X_5^i \, Y_{j+1,k}^{i+1/2} \qquad (4.2)$$

where Y is a dummy variable for w, $\xi$, and T. Q is the source term. The expressions for Q and the coefficients associated with the variables w, $\xi$, and T are given below :

Coefficients of w

$X_1 = C/2\Delta r - 1/(\Delta r)^2$

$X_3 = 2/(\Delta r)^2$

$X_5 = -C/2\Delta r - 1/(\Delta r)^2$

$X_2 = -B/2\Delta\phi - 1/(r\ \Delta\phi)^2$

$X_4 = B/2\Delta\phi - 1/(r\ \Delta\phi)^2$

$X_6 = 2/(r\ \Delta\phi)^2$

$Q = -1/R \ \ \cos\alpha \ \partial P/\partial\theta$

Coefficients of $\xi$

$X_1 = C/2\Delta r - 1/(\Delta r)^2$

$X_3 = 2/(\Delta r)^2$

$X_5 = -C/2\Delta r - 1/(\Delta r)^2$

$X_2 = -B/2\Delta\phi - 1/(r\ \Delta\phi)^2$

$X_4 = B/2\Delta\phi - 1/(r\ \Delta\phi)^2$

$X_6 = 2/(r\ \Delta\phi)^2$

$Q = D_w$

Coefficients of T

$X_1 = A_T/2\Delta r + 1/(\Delta r)^2$

$X_3 = -2/(\Delta r)^2$

$X_5 = -A_T/2\Delta r + 1/(\Delta r)^2$

$X_2 = -B_T/2\Delta\phi + 1/(r\ \Delta\phi)^2$

$X_4 = B_T/2\Delta\phi + 1/(r\ \Delta\phi)^2$

$X_6 = -2/(r\ \Delta\phi)^2$

$Q = -w\ T/T_c$

where

$A_T = Pr\ v/r$

$B_T = 1/r + Pr\ u$

The finite difference form of the vorticity equation suitable for the SOR method is given below :

$$Z_1\psi_{j-1,k} + Z_2\psi_{j,k-1} + Z_3\psi_{j,k} + Z_4\psi_{j,k-1} + Z_5\ \psi_{j+1,k} = r^2\Delta r\ \xi_{j,k} \qquad (4.3)$$

where :

$Z_1 = r^2 \left[ 1/2r + 1/\Delta r \right]$

$Z_2 = \Delta r/(\Delta\phi)^2$

$Z_3 = -2 \left[ r^2/\Delta r + \Delta r/(\Delta\phi)^2 \right]$

$Z_4 = \Delta r/(\Delta\phi)^2$

$Z_5 = r^2 \left[ -1/2r + 1/\Delta r \right]$

## 4.4 NUMERICAL PROCEDURE

In this study, where steady and fully developed velocity and temperature fields are assumed, the governing equations are two-dimensional , i.e. flow variables may vary just in two directions; the radial r and the tangential $\phi$, and so , according to the ADI method, iteration step is split into two halves.

The numerical procedure followed to accomplish this work is described as follows:

1) Due to symmetry, the domain of interest is, just, the upper half of the tube cross-section. This domain is to be prepared for finite difference operations, and so it is divided into 20 equally spaced intervals in both r and $\phi$ directions, resulting in a 21 21 grid, ( see figure 4-1 ).

2) An initial guess is given for all dependent variables under consideration ( i.e. v, $\xi$, $\psi$ and T ) at all points in the domain of interest. Reasonable initial guess decreases computation time. For example, parabolic axial velocity profile for a given axial pressure gradient leads to significant reduction in computation time when solving flow field equations.

3) The parabolic governing equations ( Equations 3-11, 3-12, and 3-13 ) are put in their finite difference form according to the ADI method. Either derivatives with respect to r or $\phi$ can be put implicitly in the first half of the iteration step. In this study, derivatives with respect to r

are put implicitly in the first half of iteration step. The rest of the terms in the governing equations are put explicitly ( depending on their initial values). The result of this process is a linear system of equations that form a tri-diagonal matrix, which is relatively easy to solve, and which is also one of the advantages of the ADI method.

4) The solution obtained from step 3 is considered initial guess for the solution of the second half of the iteration . In this second half, derivatives with respect to $\phi$ are put implicitly and other terms of the governing equations are put explicitly, resulting in a tri-diagonal matrix , and can be solved easily.

5) The procedure mentioned in both (3) and (4) above was applied first to the axial velocity equation. The resulted new axial velocity field was introduced into the secondary flow equation, and then the procedure of ( 3 ) and ( 4 ) was applied successively.

6) The resulted new field of $\xi$ from ( 4 ) is used in solving Equation 3-8 using SOR method to calculate $\psi$.

7) w, $\xi$, and $\psi$ which result after a complete iteration are considered as initial guesses for the next iteration.

8) Iterations are repeated as described above until a converged solution is obtained. A solution is considered converged when :

$$\max \left| \frac{Y^{i+1} - Y^{i}}{Y^{i+1}} \right| < 10^{-5}$$

where Y is a dummy variable for w, $\xi$, $\psi$, and T, and $i$ is the number of iteration.

9) When a converged flow solution is obtained, it is introduced into the energy equation, which is solved in the same way described above.

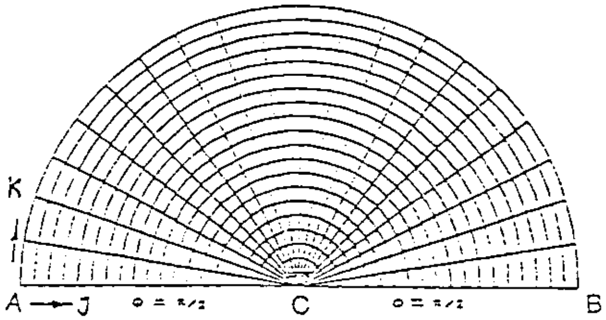


Figure 4.1 Numerical grid

## 4.5 MAJOR DIFFICULTIES IN THE NUMERICAL SOLUTION

### 4.5.1 DIFFICULTIES CAUSED BY DERIVATIVE BOUNDARY CONDITION

The discussion of the difficulties in the numerical solution caused by derivative boundary conditions is divided into three parts :

1) The following three approximations of the derivative boundary value of $\xi$ at the wall, $\xi=\partial^2\psi/\partial r^2$, were tested :

$$\xi_{1,k}= 1/2(\Delta r)^2(4\ \psi_{2,k}) \quad + o \quad (\Delta r)^2 \qquad (4.4)$$

$$\xi_{1,k}= 1/2(\Delta r)^2(8\ \psi_{2,k}- \ \psi_{3,\ k}) + o\ (\Delta r)^2 \qquad (4.5)$$

$$\xi_{1,k}= 1/2(\Delta r)^2(12\ \psi_{2,k} - 3\ \psi_{3\ ,k}+ \frac{4}{9}\psi_{4,k})\ o\ (\Delta r)^3 \qquad (4.6)$$

The first approximation, which was given in the pioneering work of Thom and has been used extensively since then , leads to more stable solutions

2) The derivative boundary condition of both w and T at the center point : When solving the equation of the first half of iteration ( Eq. 4-1 ) for both w and T, it is necessary to know both w and n values at the center point in advance as boundary conditions. These boundary values are obtained from initial guess, or from the previous iteration half step. A good technique followed which gives modified values for both w and T at the center point is adopted. This

technique simply solves v and T equations along the vertical diameter. Then the new values obtained of both v and T at the center point can be considered as good boundary values for the first half iteration ( i.e., for Equation 4-1 which is implicit in r-direction ). For the second half iteration, the values of v and T at the center point are those updated from the solution of the first half step iteration.

3) The derivative boundary condition of both v and T along the horizontal diameter : At the left half of the horizontal diameter, i.e., $\phi = -90^\circ$, forward differences are used for the derivative boundary conditions $\partial v/\partial\phi = 0$ and $\partial T/\partial\phi = 0$ which are given as follows :

$$\partial Y/\partial\phi = 1/(2\Delta\phi)\ (-3\ Y_{j,1} + 4\ Y_{j,2} - Y_{j,3})$$

where Y is a dummy variable for v and T.

On the other hand, along the right side of the horizontal diameter, i.e. $\phi = 90^\circ$, backward differences are used for the derivative boundary conditions : $\partial v/\partial\phi = 0$ and, $\partial T/\partial\phi = 0$ which are given as follows :

$$\partial Y/\partial\phi = 1/(2\Delta\phi)\ (3\ Y_{j,21} - 4\ Y_{j,20} + Y_{j,19})$$

### 4.5.2 Difficulties of convergence of solution

The finite difference equations ( 4-1 ) and ( 4-2 ), with their boundary conditions, each form a set of equations in the following general form :

$$\alpha^{i} Y^{i+1} = \beta^{i} \tag{4.7}$$

where $\alpha^{i}$ is a tridiagonal matrix and is a function of the stream function, coordinates, and grid spacings. $\alpha^{i}$ was found to be diagonally not dominant. This caused the solution of Eq. 4-7 to diverge. To overcome this difficulty, the following technique has been adopted : A convergence parameter, $\lambda$ , is introduced into Eq. (4-7), so that $\alpha$ becomes diagonally dominant. This is done as follows :

$$( \alpha^{i} + \lambda I ) Y^{i+1} = \beta^{i} + \lambda I Y^{i} \tag{4.8}$$

$\lambda$ is taken to be a multiple of the middle element in the main diagonal of the tri-diagonal matrix $\alpha^{i}$. I is the unity matrix.

The range of $\lambda$ used in this study for the solution of w equation was from about 5 to about 10. For secondary flow equation $\lambda$ ranges from about 5 to about 20. For the energy equation the range of $\lambda$ is from 5 t0 20 for values of Pr from .05 to 5.0. Higher values of Pr required $\lambda$ values up to 60 for Pr of 40 .

# CHAPTER 5

# RESULTS AND DISCUSSIONS

## 5.1 FLUID FLOW RESULTS

The effect of coil curvature on fluid flow is manifested through the induced centrifugal forces acting on fluid particles. A pressure gradient in the direction toward the center of curvature is induced to balance these forces, and consequently form a pressure field with maximum value at the outer most point of the tube cross-section (at $\phi = 90^\circ$, see figure 3-1). The pressure near the wall decreases circumferentially going from the outer side to the inner side of the tube cross-section, due to the fact that centrifugal forces acting on fluid particles close to the wall decrease as moving closer to the coil center. This will cause pressure field near the wall to behave as if there is a vacuum side in the range of $\phi$ from $0^\circ$ to $-90^\circ$, and a pressure side from $90^\circ$ to $0^\circ$. The fluid close to the wall will move counterclockwise from higher pressure regions to lower pressure regions, hence, secondary motion will be induced in both halves of the tube cross-section. The mirror image of secondary motion in both halves of the tube cross-section holds when buoyancy effects are neglected.

As can be seen from figures (5-1) and (5-2), the stream lines show how tangential velocity varies across the tube cross-section. According to the definitions of the tangential velocity component, the places in which streamlines are very close to each other indicate high tangential velocities.

Figures 5-3 and 5-4 show the axial velocity profile along the horizontal diameter. The distortion from the parabolic profile of flows in straight horizontal tubes is clear. This is due to centrifugal forces acting on fluid particles. The greater the pressure gradient, the greater the shift of the point of maximum axial velocity towards the outer side of the tube.

## 5.2 Heat transfer results

Results of the thermal side of this study are given in terms of the followings : 1) Dimensionless temperature contours, 2) Local Nusselt number profiles as a function of angular position along the circumference for different Prandtl numbers and different inclination angles of the tube axis $\alpha$ (i.e different coil pitches), and 3) In terms of peripherally averaged Nusselt number as function of coil pitch angle $\alpha$ for different Prandtl numbers.

### 5.2.1 Discussion of temperature contours

The discussion is divided into three parts, the first concerns low Prandtl number. The second and third concern high and intermediate Prandtl number respectively.

1) Low Prandtl number ( Pr = 0.05 ):

Figures 5-5, 5-6, show the dimensionless temperature contours for Prandtl number of 0.05 and for two flow situations ( low and intermediate Dean numbers). They all have very similar shapes, but differ in the values of the difference in magnitude between each two adjacent lines, i.e. $\Delta T$ .These figures show that the point of maximum dimensionless temperature, although shifted towards the outer side of the tube cross-section, lie along the horizontal diameter. The maximum dimensionless temperature corresponds to the hotest or coldest temperature, depending on whether the process considered is cooling or heating. For low Prandtl number fluids, e.g. liquid metals, conduction mode of heat transfer is more important than convection. This will cause a smooth variation in temperature across the tube cross-section. This result can be seen by noting the relatively uniformly spaced temperature contours, compared with the situation of high Prandtl number temperature contours shown in figures 5-7 to 5-10 .

2) High Prandtl number ($5.0 \le Pr \le 40$) :

Figures 5-7 to 5-10 show that the point of maximum dimensionless temperature is shifted off the horizontal diameter, ( causing double maxima to appear when considering both the upper and lower halves of the tube cross-section ). For low De the angular position of the maximum dimensionless temperature is near $\phi = 0°$. The greater the Dean number the greater the shift towards the inner surface of the tube. For high Prandtl number fluids, the convective heat transfer mode is dominant. This can be realized by noting the steep variations in temperature in figures 5-7 to 5-10, especially in the vicinity of the wall in the range of $\phi > 0°$.

Large portion of the high Pr fluid entering the central region from the inner side of the tube cross-section has been heated ( or cooled ) to temperatures close to that of the wall, as a result of secondary motion. This will cause central region temperature to be not far removed from that of the wall.

Temperature contours shown in figures 5-9 and 5-10, correspond to Pr of 25 and 40 respectively. In addition to what is mentioned above, these figures show that some peaks appear near the wall at $\phi = 90^{\circ}$.

3) Intermediate Prandtl number ( Pr = 1.0 ) :

For intermediate values of Pr, temperature contours have characteristics of low Pr temperature contours. The point of maximum dimensionless temperature is still on the horizontal diameter. But because of more convection contributing to heat transfer, it is shifted more to the outer bend of the tube than that in the case of low Pr. These situations are shown in figures 5-11 and 5-12 .

### 5.2.2 Local Nusselt number Nu

For intermediate and high Prandtl numbers the variation of Nu along the circumference is significant. On the other hand for low Prandtl number the variation of Nu is not so important. These situations are shown in figures 5-13, to 5-20.

The minimum value of local Nu for all Pr and all De was found to be always at the inner most angular position, i.e. at $\phi = -90^{\circ}$. In fact, Nu at $\phi = -90^{\circ}$ was found to be less than that of horizontal straight tubes, i.e. less than 3.66. This can be explained by recalling that the fluid in the vicinity of the inner wall is at temperatures relatively close to the wall temperature, due to the secondary flow which has passed near the wall and has been heated ( or cooled ) close to the wall temperature.

### 5.2.3 Peripherally averaged Nusselt number

Average Nusselt number results are given as functions of $\alpha$. These results are shown in figures 5-21, to 5-24. As shown in these figures the variation of $\overline{Nu}$ with pitch angle $\alpha$ is negligible up to values of $\alpha$ of about $30^{\circ}$. For values of $\alpha$ greater than about $30^{\circ}$ the decline in $\overline{Nu}$ profile is clear. The variation of De with $\alpha$ is also presented in figures 5-21 to 5-23, where up to $\alpha$ of about $30^{\circ}$ the reduction in De is small. Further increase in $\alpha$ results in a considerable reduction in De.

Average Nusselt number, $\overline{Nu}$ ,as a function of De for different Prandtl number values is shown in figures 5-25 and 5-26 .

Over the studied range of De, i.e. approximately $60 < De < 400$ and for Pr of both 1.0 and 5.0, the average Nusselt number is correlated by the following correlation :

$$\overline{Nu} = 0.856\ De^{0.5094}\ Pr^{0.1143} \qquad (5\text{-}1)$$

Table 5.1 shows : 1) $\overline{Nu}$ values that are used to make the correlation given in Eq. 5-1, 2) $\overline{Nu}$ values that resulted from Eq. 5-1, and 3) the deviation between $\overline{Nu}$ obtained both numerically and from Eq. 5-1.

Table 5.1 : Numerical and correlation average Nusselt number results

| De | Pr | $\overline{Nu}$ Numerical | $\overline{Nu}$ correlation 5.1 | Deviation % |
|---|---|---|---|---|
| 67.0 | 1 | 7.00 | 7.29 | 4.10 |
| 73.1 | 1 | 7.66 | 7.62 | 4.50 |
| 308.3 | = | 15.18 | 15.86 | 4.50 |
| 328.0 | = | 17.19 | 16.37 | 4.80 |
| 67.0 | 5 | 8.61 | 8.76 | 1.70 |
| 73.0 | 5 | 9.25 | 9.16 | 1.02 |
| 308.3 | = | 17.75 | 19.06 | 7.40 |
| 328.0 | = | 19.79 | 19.67 | 0.60 |

## 5.3 Effect of coil pitch on fluid flow and heat transfer in helical coils

For the same curvature ratio and the same $\partial p/\partial\theta$, increasing the pitch angle $\alpha$ will result in the damping of secondary motion. Although $\partial P/\partial\theta$ is the same, the pressure gradient along the tube axis, i.e. $\partial P/\partial L$ is decreased. $\partial P/\partial L$ is related to $\partial P/\partial\theta$ by the following relation

$$\partial P/\partial L = \cos\alpha \; \partial P/\partial x$$

where

$\partial P/\partial x$ is the axial pressure gradient when $\alpha$ is zero.

An example that shows the effect of $\alpha$ on De is given below : For R= 100, and $\partial P/\partial \theta$ = 400000, De was decreased from 73.144 to 67.0, i.e. by about 8 % , when $\alpha$ increased from $0^\circ$ to $30^\circ$. Increasing $\alpha$ up to $45^\circ$ results in decreasing De to 59.0, i.e. by about 15 % .

Decreasing the intensity of secondary motion by increasing $\alpha$ results in decreasing heat transfer by convection, which is dominant when Pr is high . For low values of Pr ( Pr =0.05 ), the effect of varying $\alpha$ is not important, since convection mode of heat transfer is not important compared with conduction mode. This can be noticed quantitatively by noting that for the same R and $\partial P/\partial \theta$ the average Nusselt number decreased by about 10 % for high and intermediate Pr, and by about 5 % for low Pr when $\alpha$ is increased from $0^\circ$ to $30^\circ$. Increasing $\alpha$ to $45^\circ$ decreases $\overline{Nu}$ by about 20 % in the case of intermediate and high Pr, and by about 10 % for low Pr. From these results it becomes clear that neglecting the effect of $\alpha$ on fluid flow and heat transfer in helically coiled tubes is justified only for $\alpha < 30^\circ$. Figures 5-21 up to 5-23 show both $\overline{Nu}$ and De as functions of $\alpha$ for Pr = 5.0, $\partial P/\partial \theta$ = 3.0E6, and R = 100. . As can be seen, up to $\alpha$ of about $30^\circ$ both $\overline{Nu}$ and De are almost uniform.

## 5.4 COMPARISON WITH OTHER WORK

Some of the obtained flow results are compared with the results obtained from the approximate relation of Murakami et. al. ( 1971 ), which gives De taking into account the effect of $\alpha$ by using modified radius of curvature of the coil. The results of this comparison is seen in table 5-2. As can be seen the deviation between Murakami's results and those of this study increase with increasing $\alpha$ . The relation of Murakami et. al. is given below :

$$De = Re \left( \frac{a}{\rho} \right)^{1/2}$$

where

$$\rho = R' ( 1 + \tan^2\alpha )$$

Thermal results are also compared with other works. Peripherally averaged Nusselt number results obtained from the correlation given in Eq. 5-1 are compared with the results obtained from the following correlations made by both Rabadi, 1989, and Kalb and Seader, 1974.

Rabadi's correlation :

$$\overline{Nu} = 0.507\, De^{0.611}\, Pr^{0.116} \qquad 100 < De < 1300, \quad 0.7 < Pr < 5.0$$

Kalb and Seader's correlation :

$$\overline{Nu} = 0.836\, De^{0.5}\, Pr^{0.1} \qquad De > 80, \quad 0.7 < Pr < 5.0$$

This comparison is shown in figures 5-24 and 5-25 . As can be seen from these figures the agreement between the results of this study and those from the correlations above is satisfactory

Table 5.2 : Comparison between Dean number calculated by Murakami's relation and that obtained in this study for R = 100

| | | De | | |
|---|---|---|---|---|
| $\alpha$ | $\partial P/\partial \theta$ | Present study | Murakami's Relation | Deviation % |
| 15 | 4.0E5 | 71.14 | 70.7 | 1.3 |
| 30 | = | 67.0 | 63.4 | 5.5 |
| 15 | 3.0E6 | 323.1 | 317.0 | 2.0 |
| 30 | = | 308.3 | 284.0 | 8.0 |

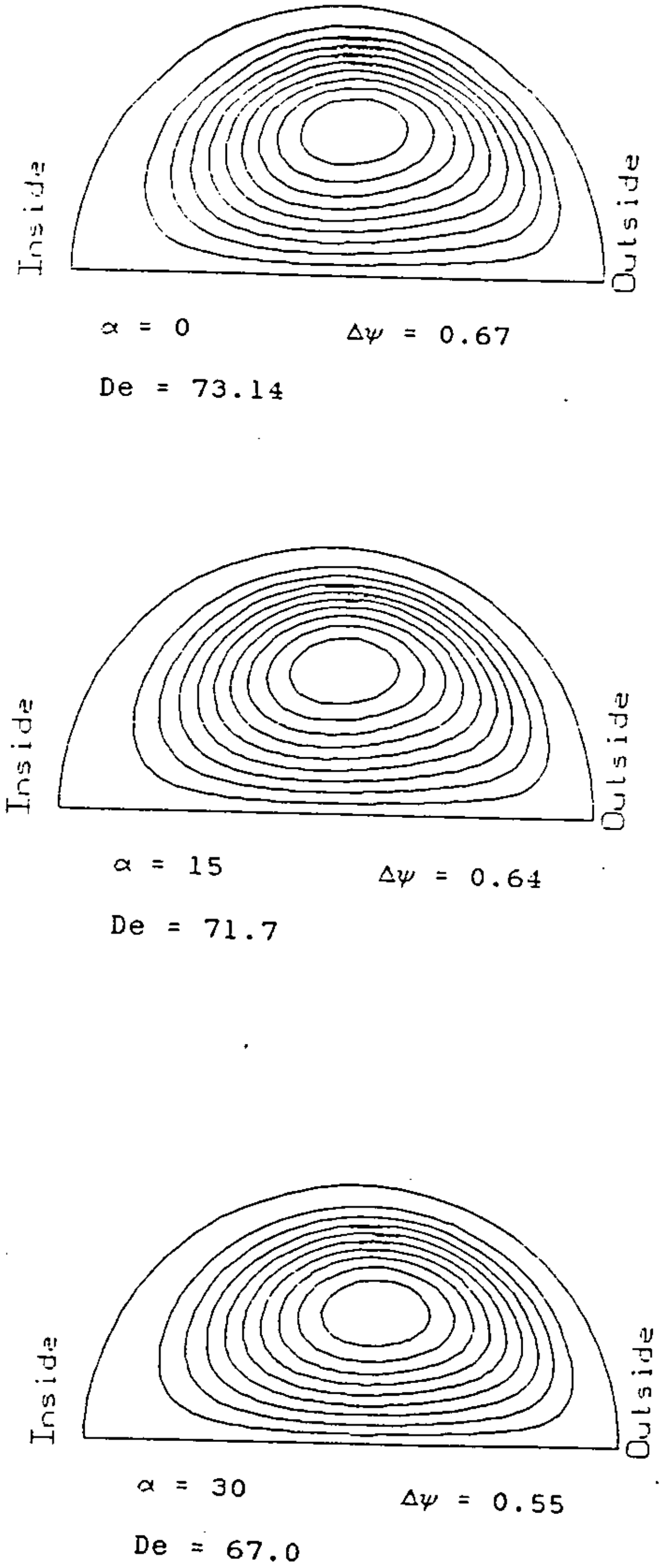


Figure (5-1) : Stream function contours for $R = 100$, and $\partial P/\partial \theta = 4.0E5$ for $\alpha = 0, 15,$ and $30$

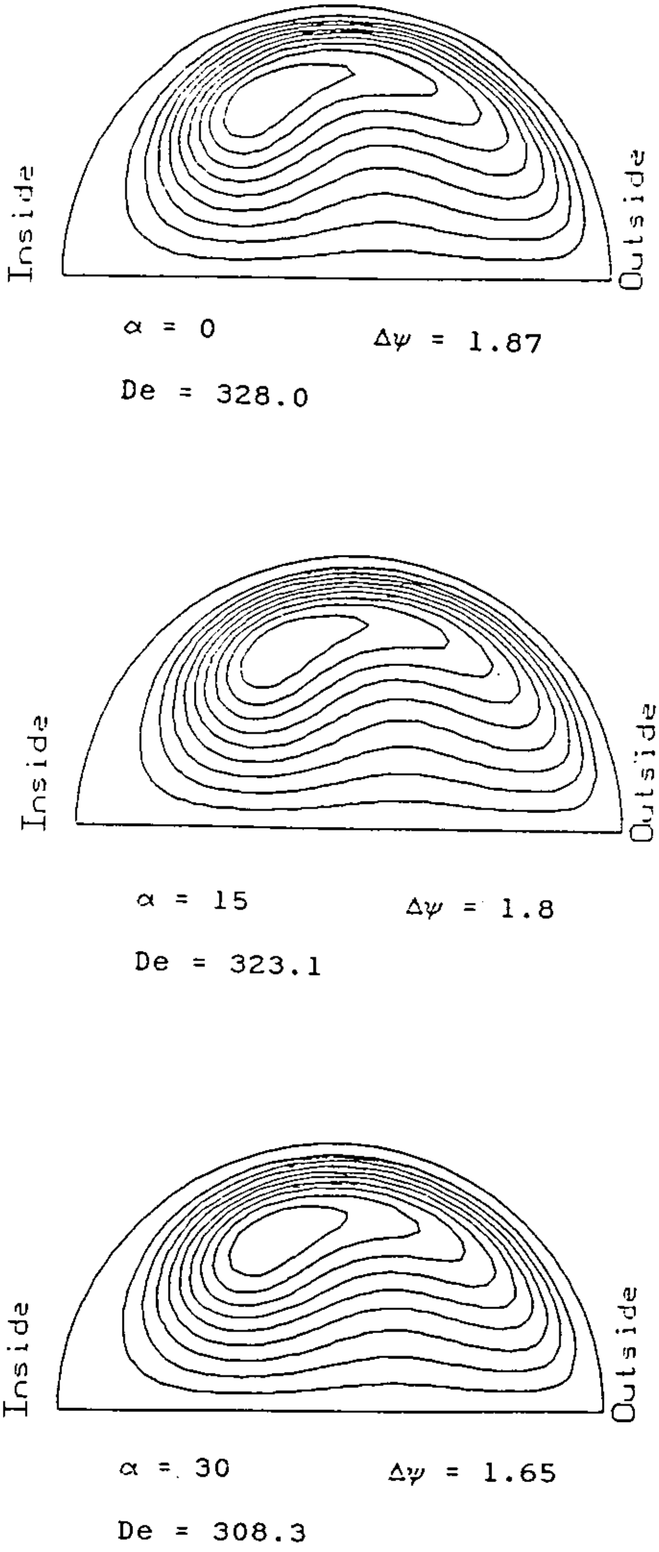


Figure (5-2) : Stream function contours for $R = 100$, and $\partial P/\partial \theta = 3.0E6$ for $\alpha = 0$, 15, and 30

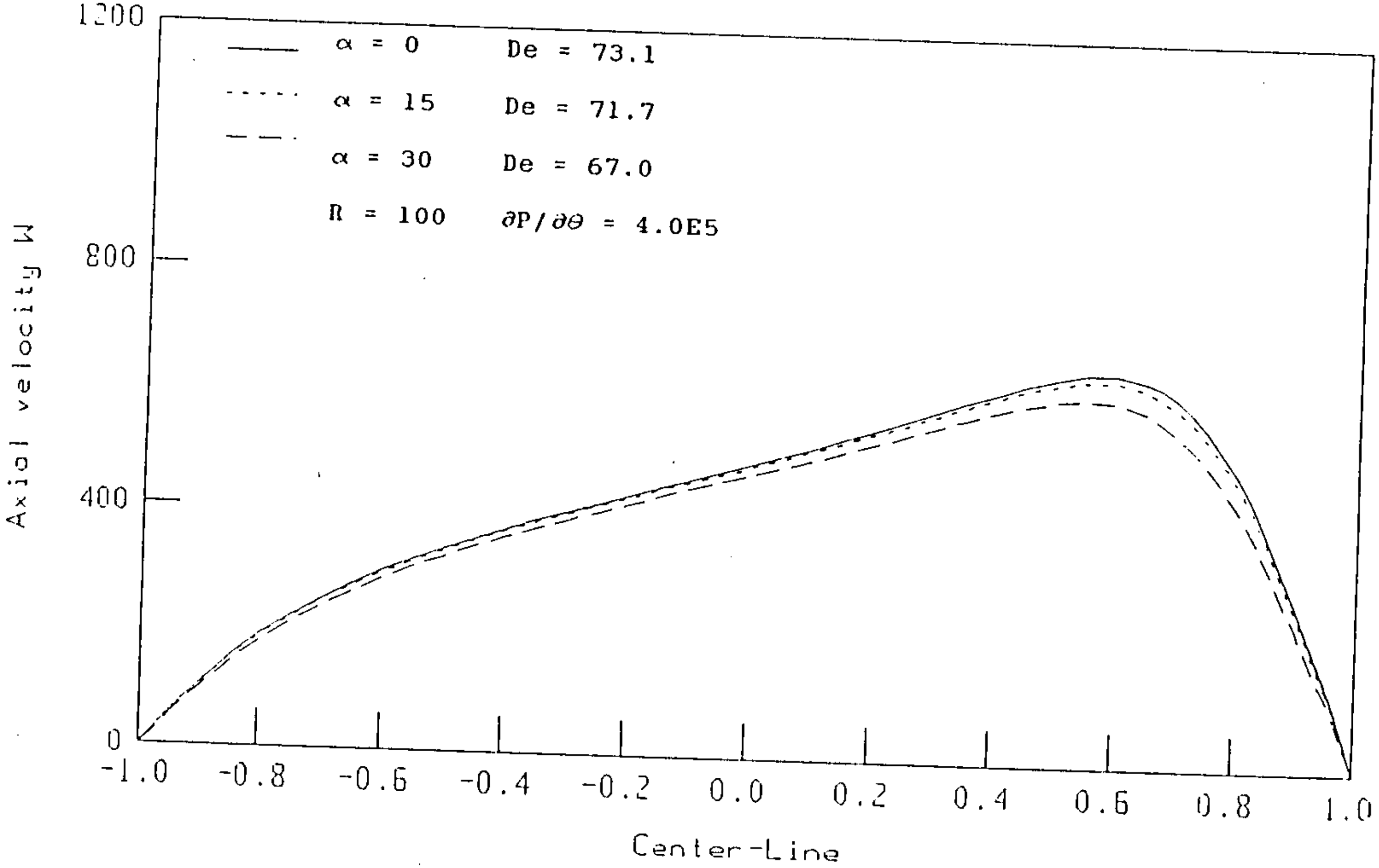


Figure (5-3) : Axial velocity profile along the horizontal diameter of the tube cross-section for different tube axis inclination angle $\alpha$

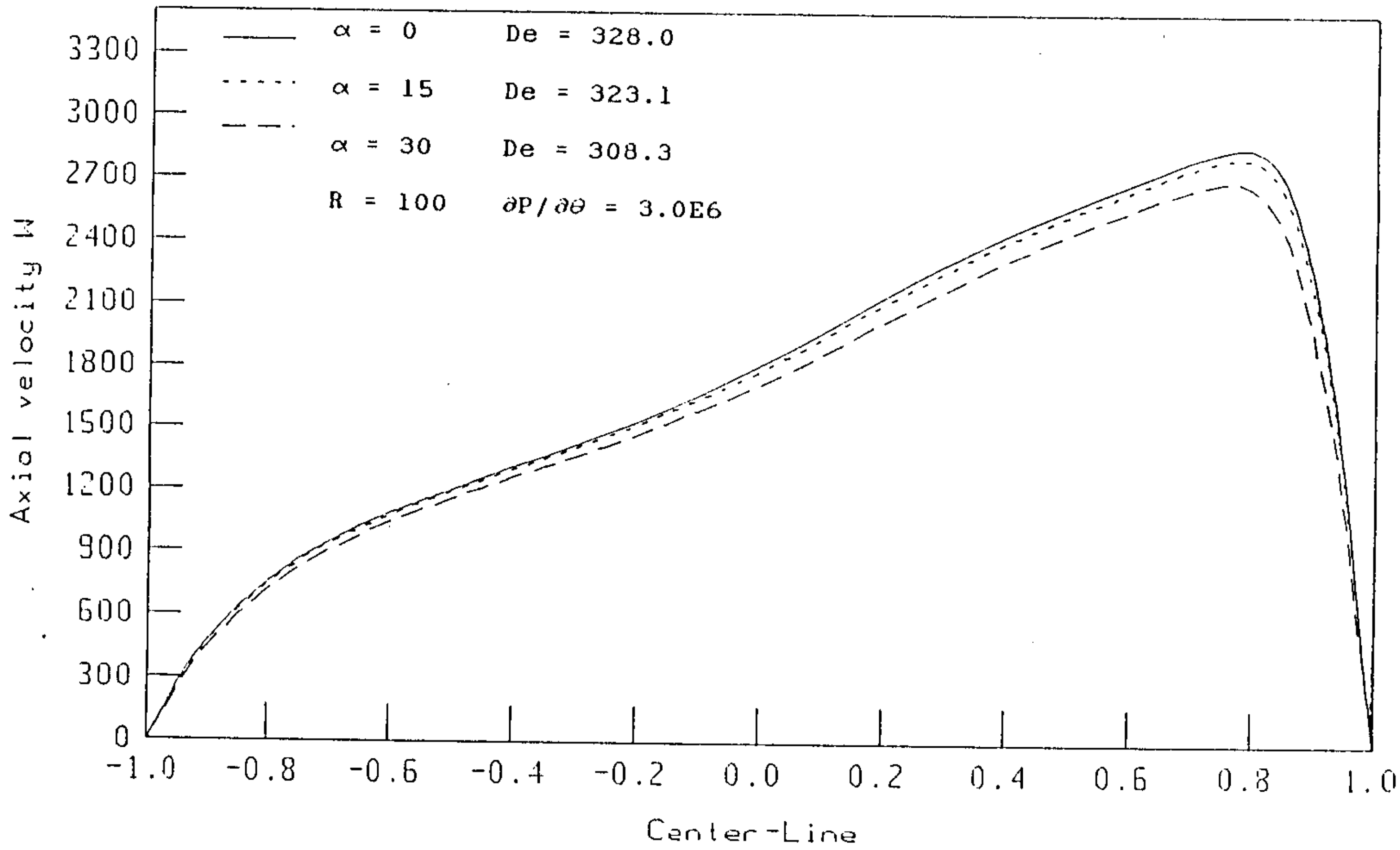


Figure (5-4) : Axial velocity profile along the horizontal diameter of the tube cross-section for different tube axis inclination angle $\alpha$

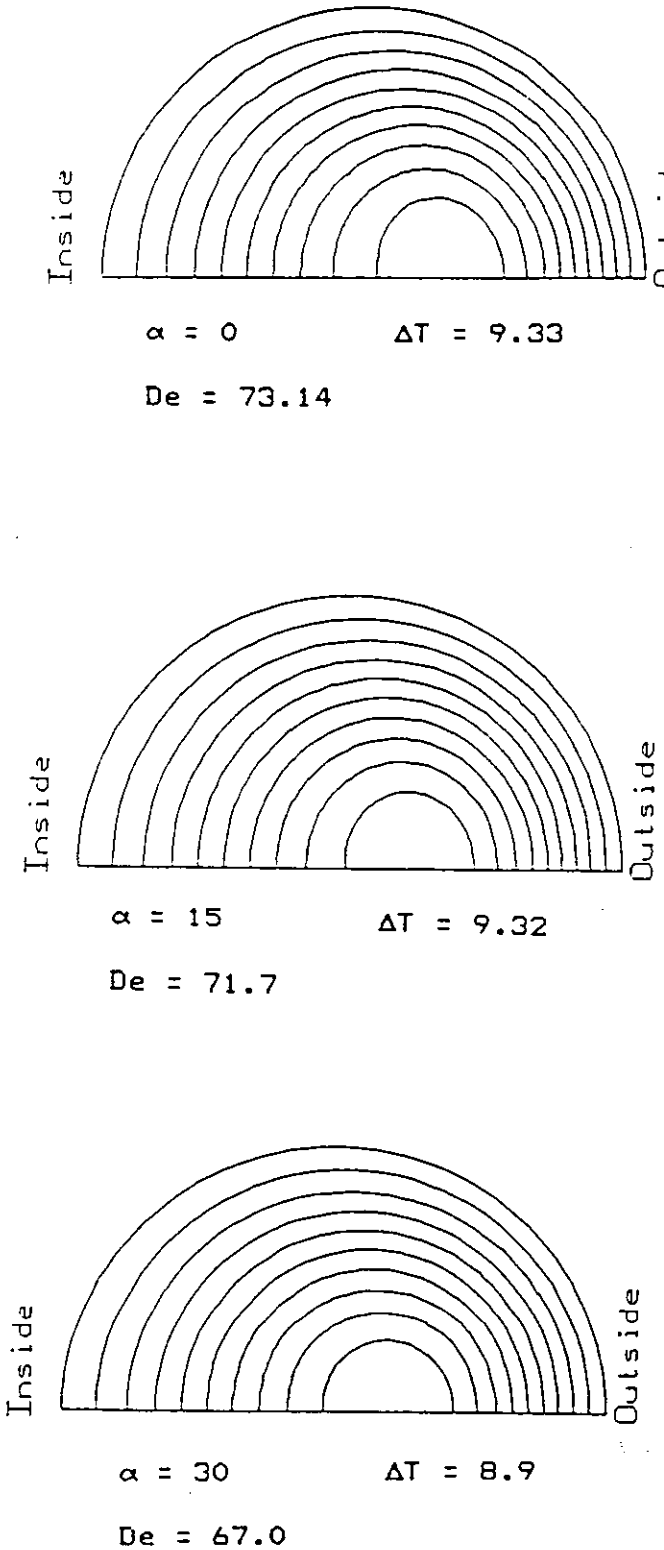


Figure (5-5): Temperature contours for $Pr = 0.05$ $R = 100$, and $\partial P/\partial\theta = 4.0E5$ for $\alpha = 0$, 15, and 30

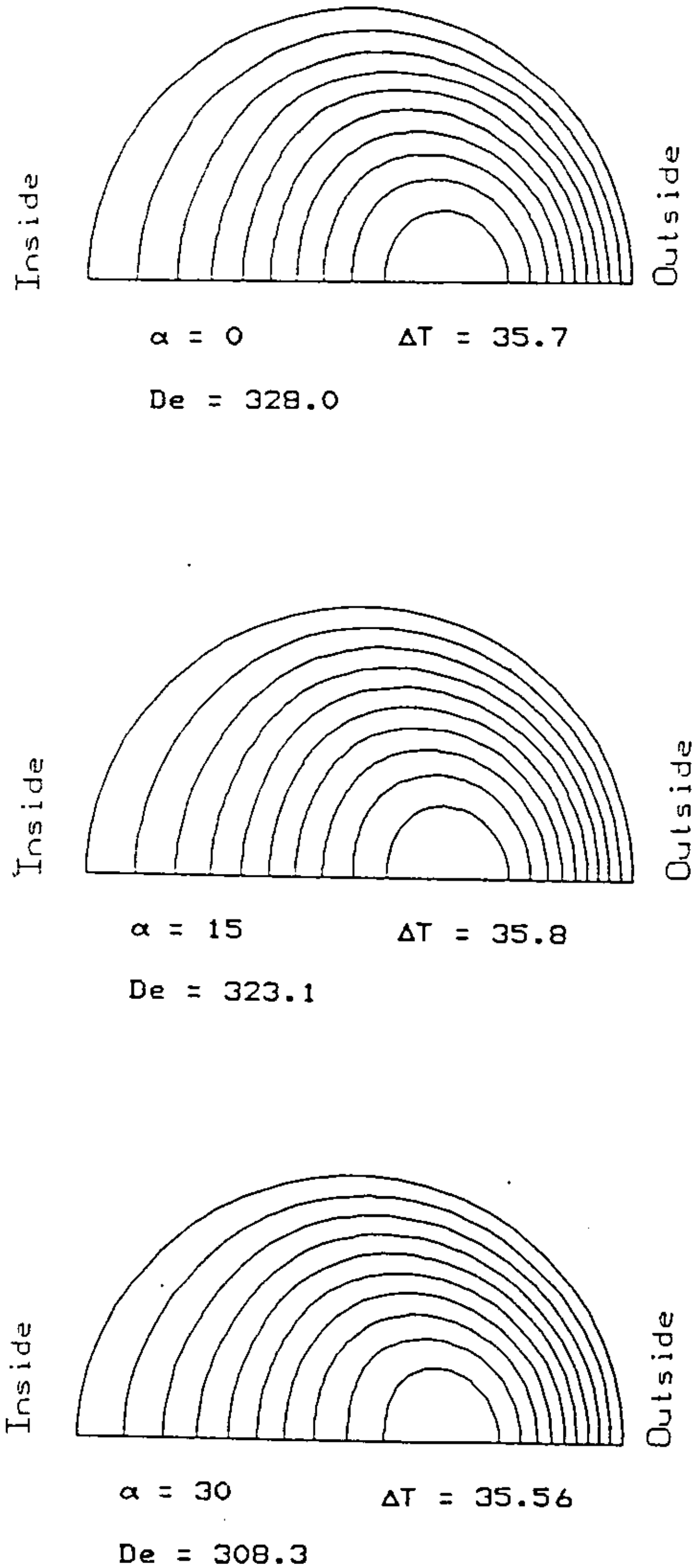


Figure (5-6): Temperature contours for Pr = 0.05 R = 100, and $\partial P/\partial\theta$ = 3.0E6 for $\alpha$ = 0, 15, and 30

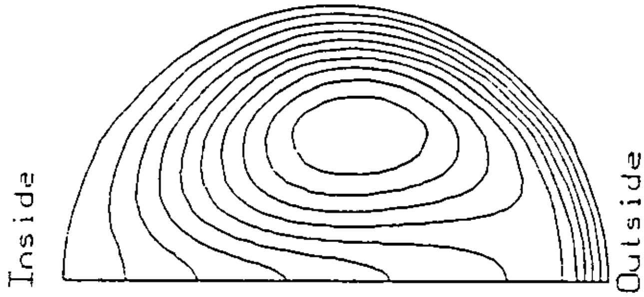


α = 0 ΔT = 11.4

De = 73.14

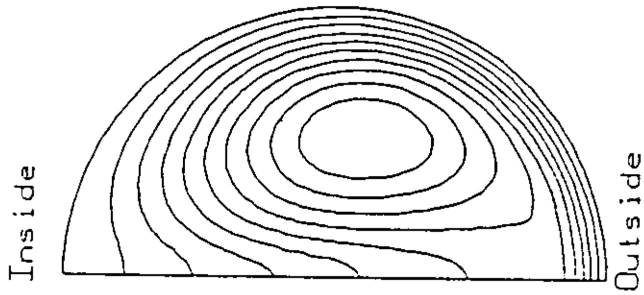


α = 15 ΔT = 11.08

De = 71.7

Figure (5-7): Temperature contours for Pr = 5.0 R = 100, and $\partial P/\partial \theta$ = 4.0E5 for α = 0, 15, and 30

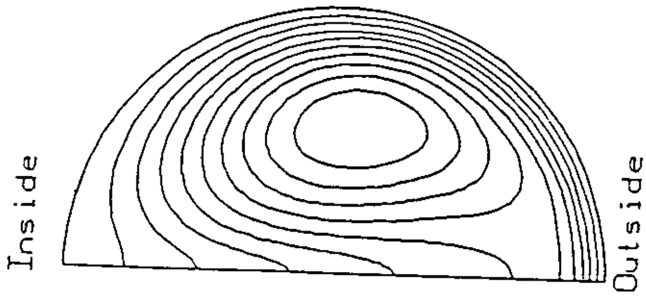


α = 30 ΔT = 10.4

De = 67.0

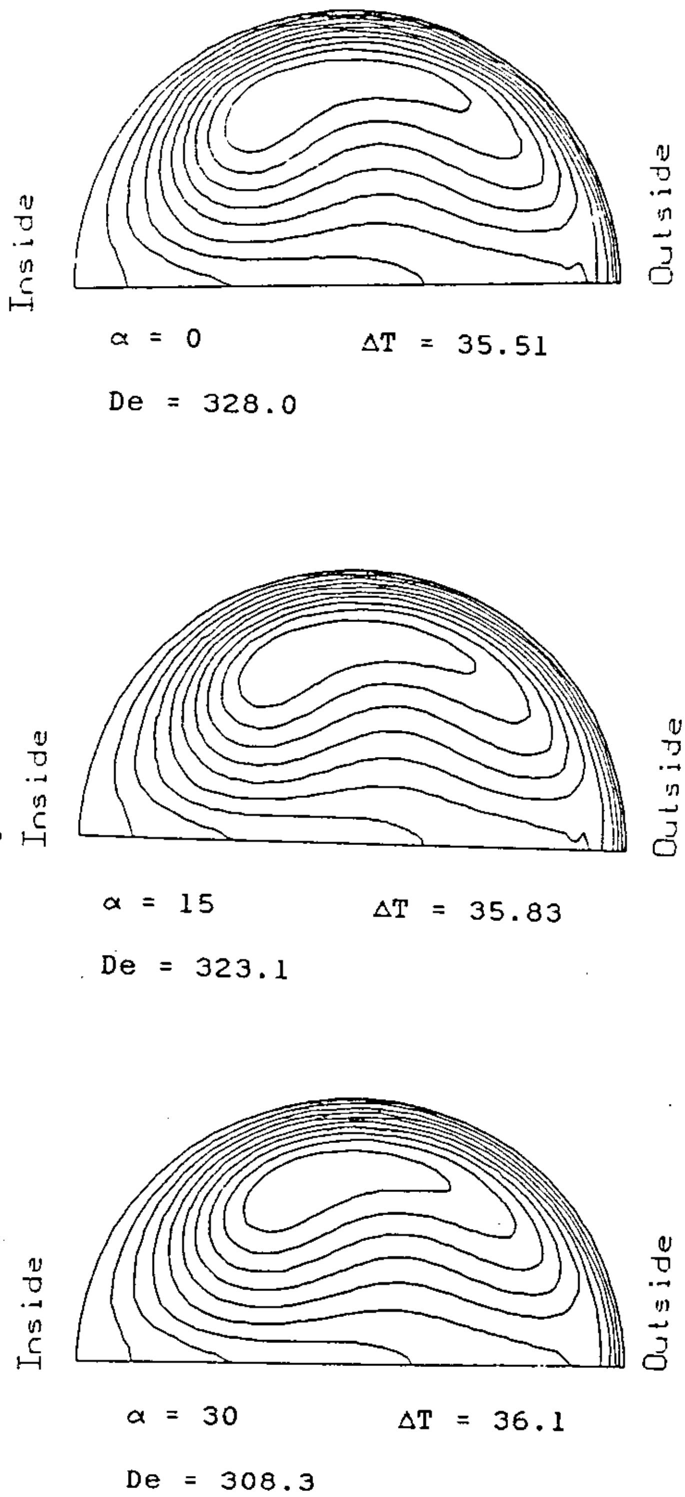


Figure (5-8): Temperature contours for Pr = 5.0 R = 100, and $\partial P/\partial \theta$ = 3.0E6 for $\alpha$ = 0, 15, and 30

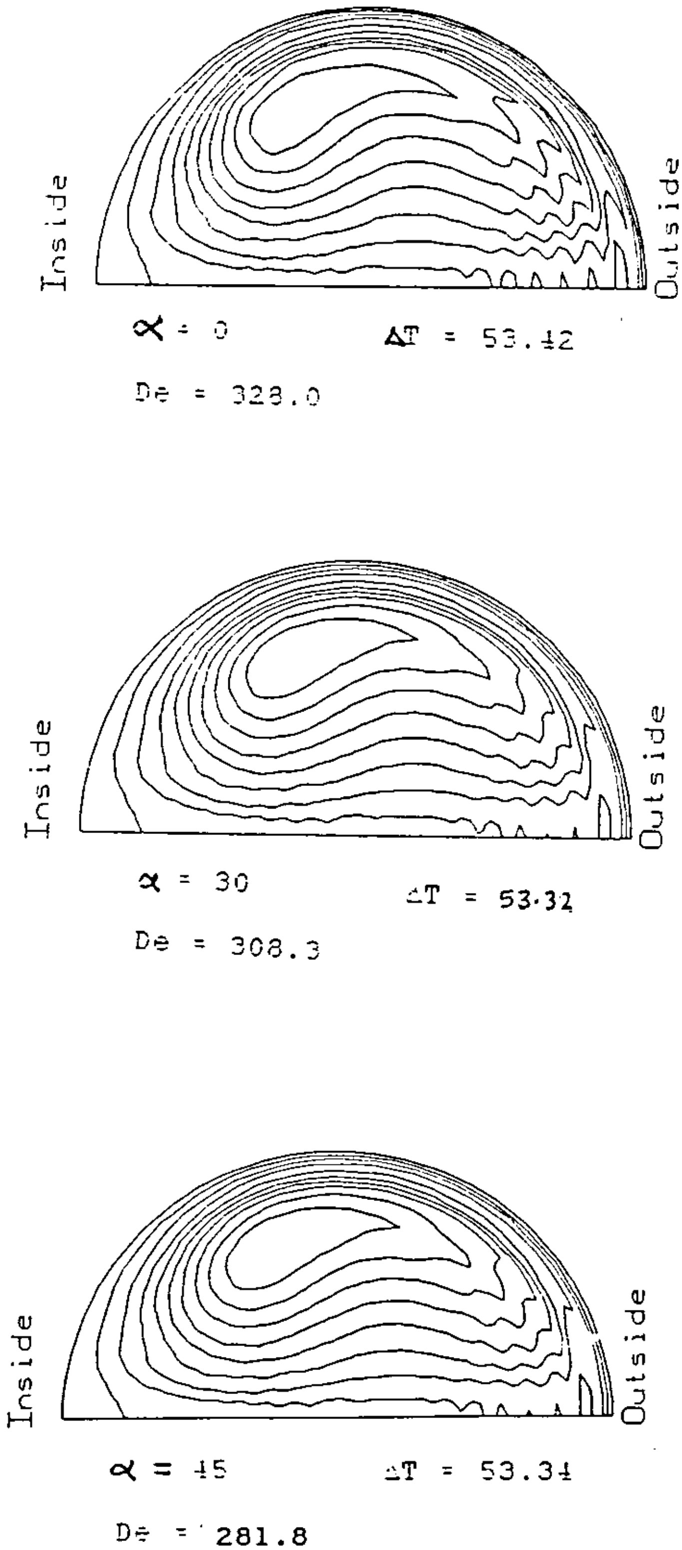


Figure (5-9): Temperature contours for Pr = 25 R = 100, and $\partial P/\partial \theta$ = 3.0E6 for $\alpha$ = 0, 30, and 45

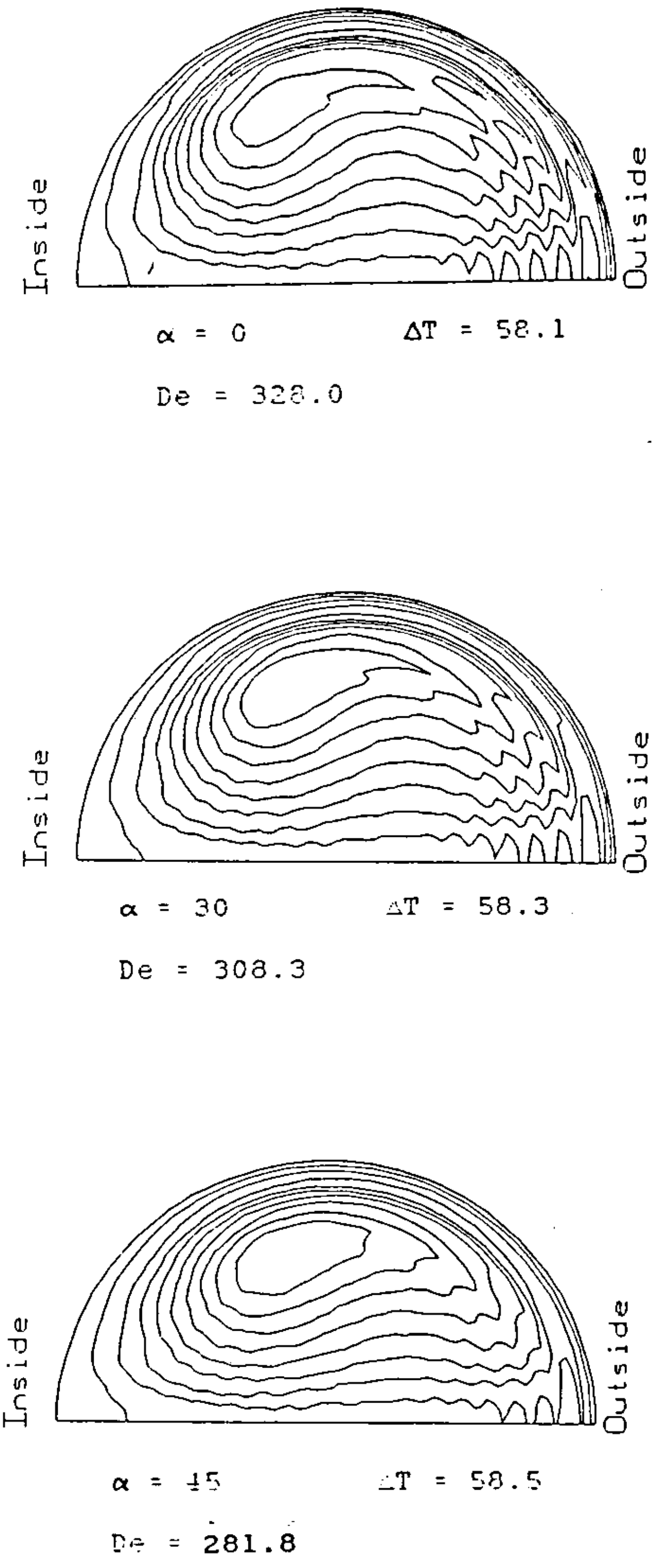


Figure (5-10): Temperature contours for Pr = 40 R = 100, and $\partial P/\partial\theta$ = 3.0E6 for $\alpha$ = 0, 30, and 45

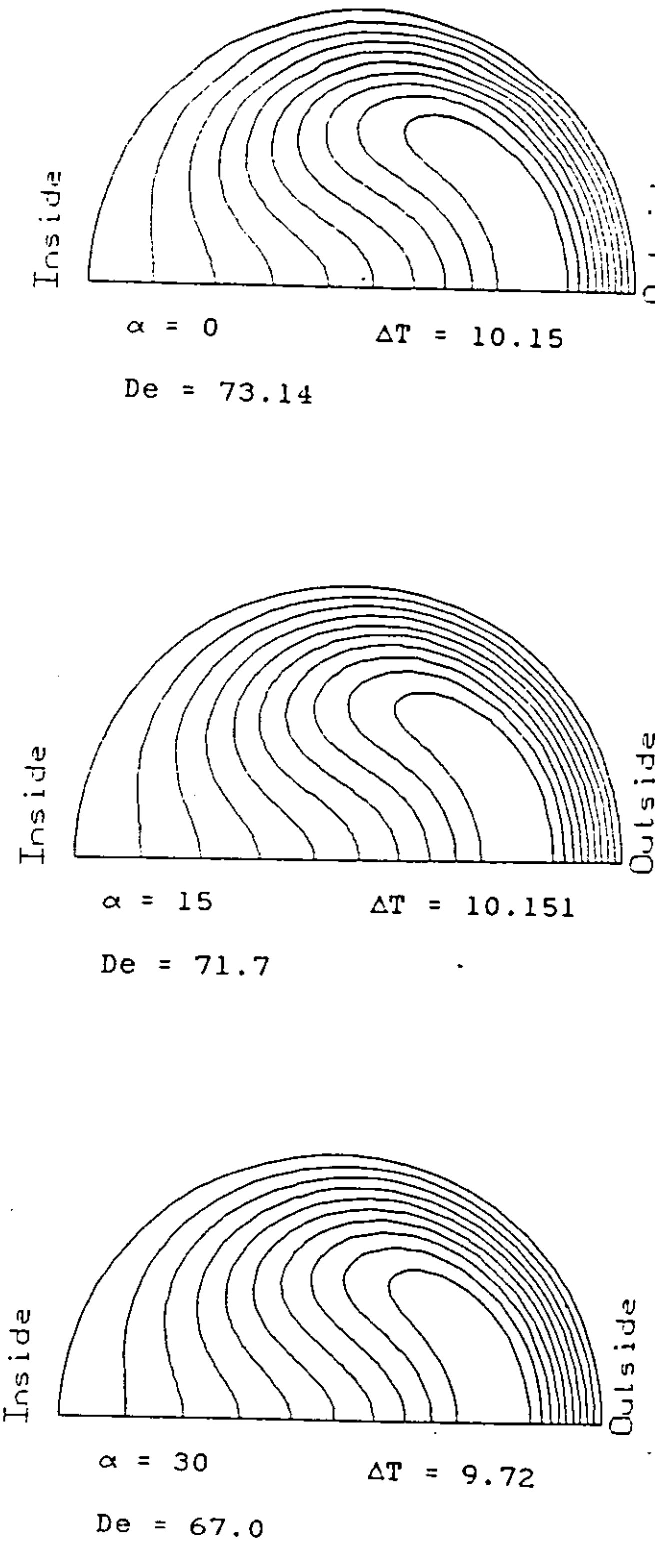


Figure (5.11): Temperature contours for $Pr = 1.0$ $R = 100$, and $\partial P/\partial \theta = 4.0E5$ for $\alpha = 0, 15,$ and $30$

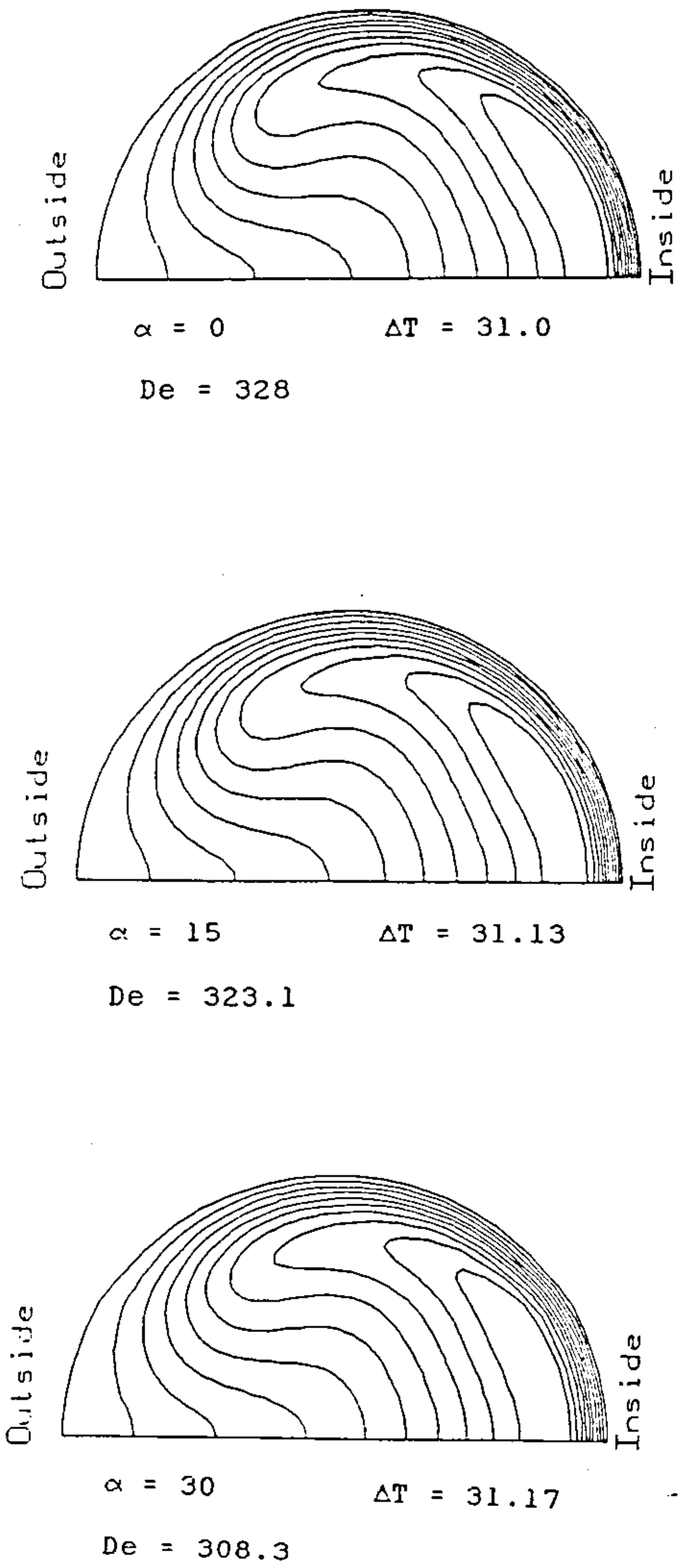


Figure (5-12): Temperature contours for Pr = 1.0 R = 100, and $\partial P/\partial \theta$ = 3.0E6 for $\alpha$ = 0, 15, and 30

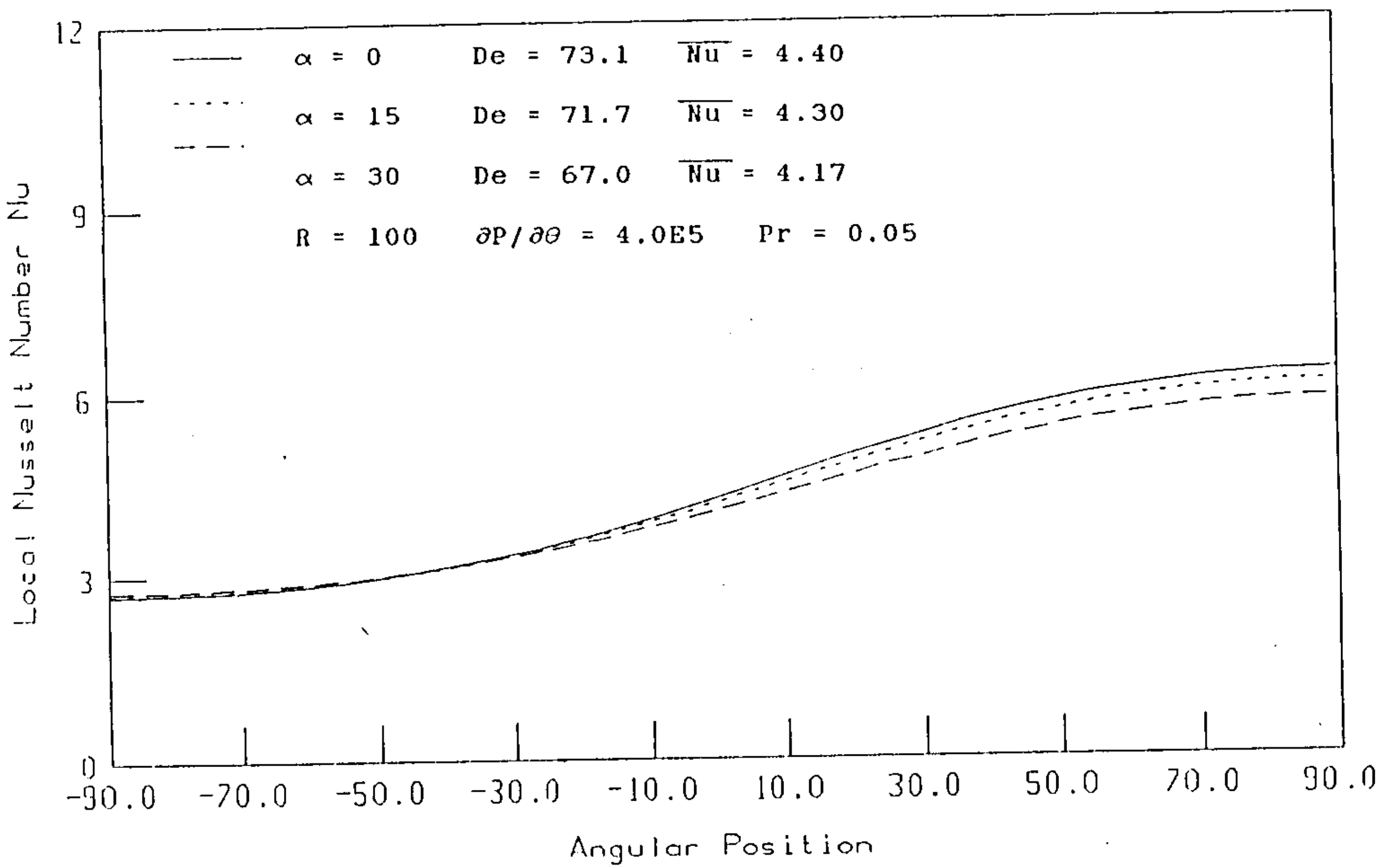


Figure (5-13) : Local Nusselt number at the wall vs angular position $\phi$

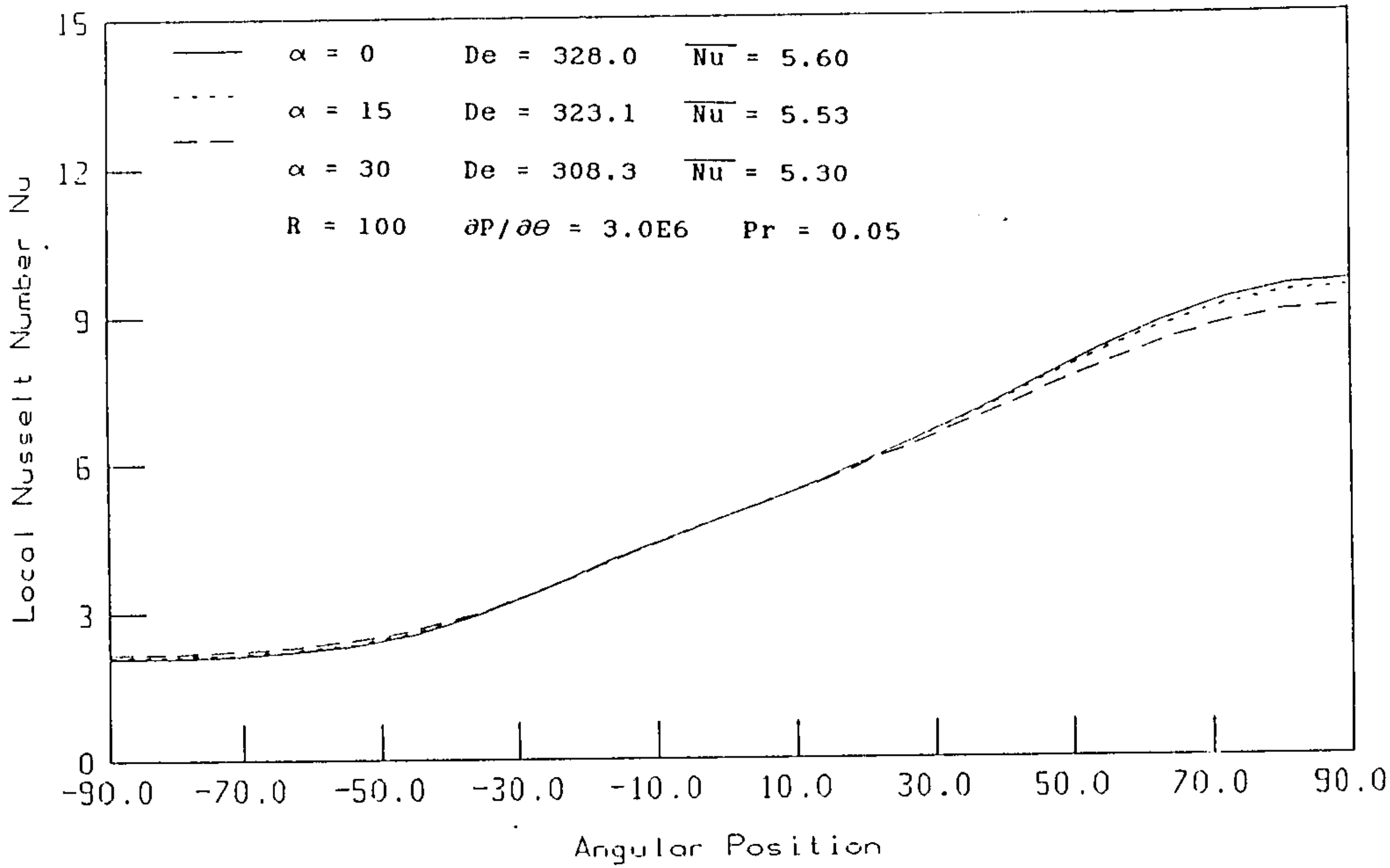


Figure (5-14) : Local Nusselt number at the wall vs angular position $\phi$

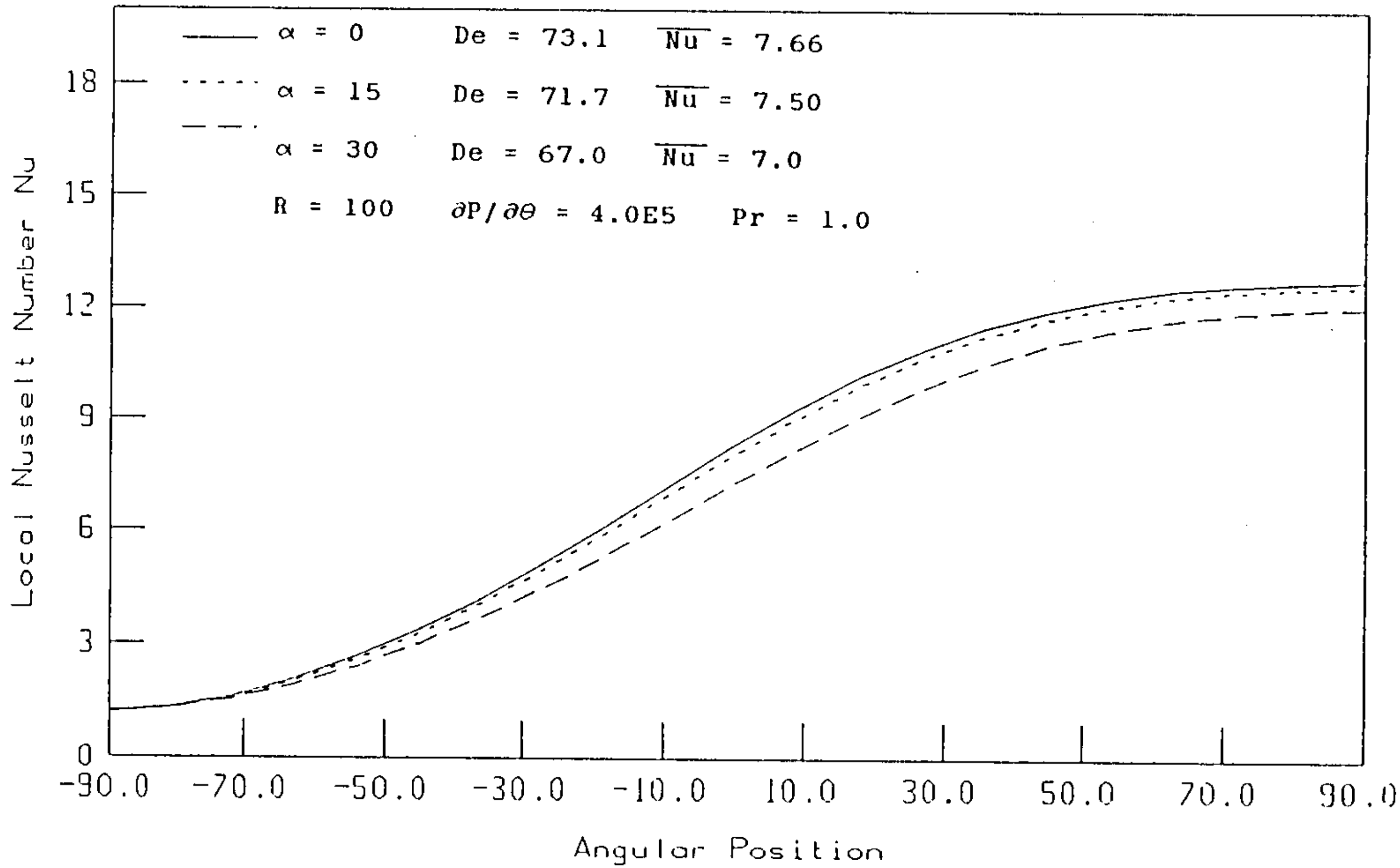


Figure (5-15) : Local Nusselt number at the wall vs angular position $\phi$

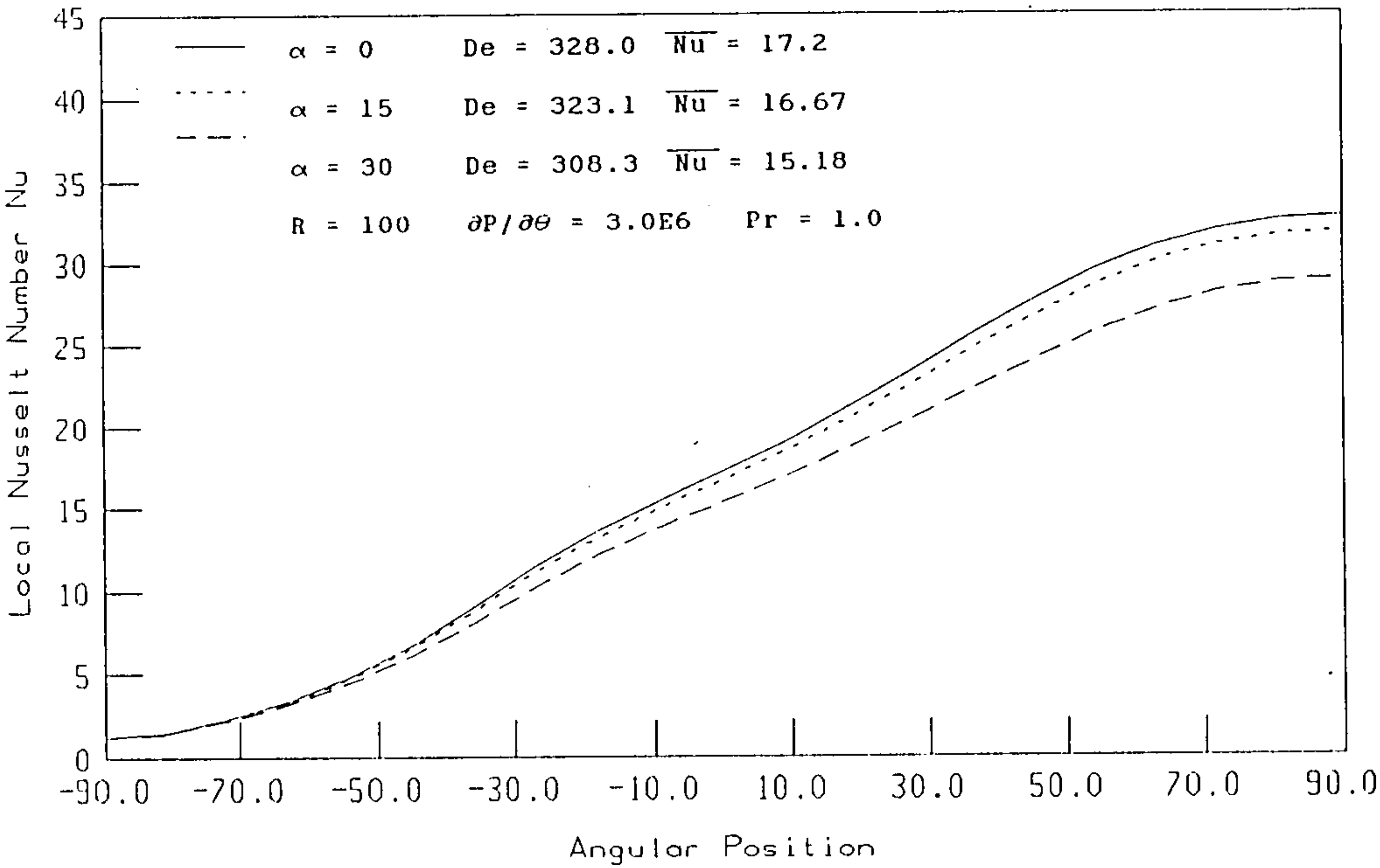


Figure (5-16) : Local Nusselt number at the wall vs angular position $\phi$

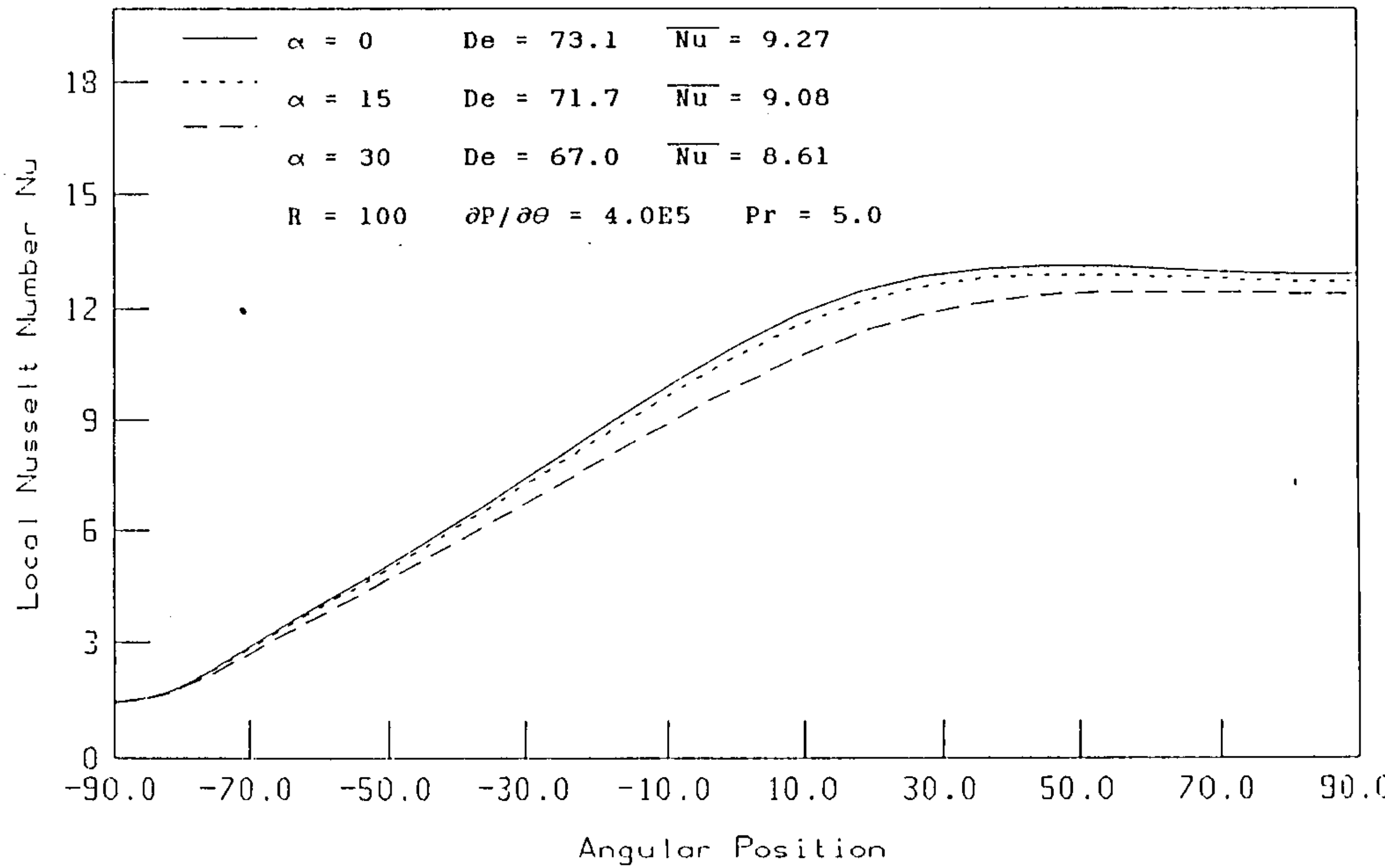


**Figure (5-17) : Local Nusselt number at the wall vs angular position $\phi$**

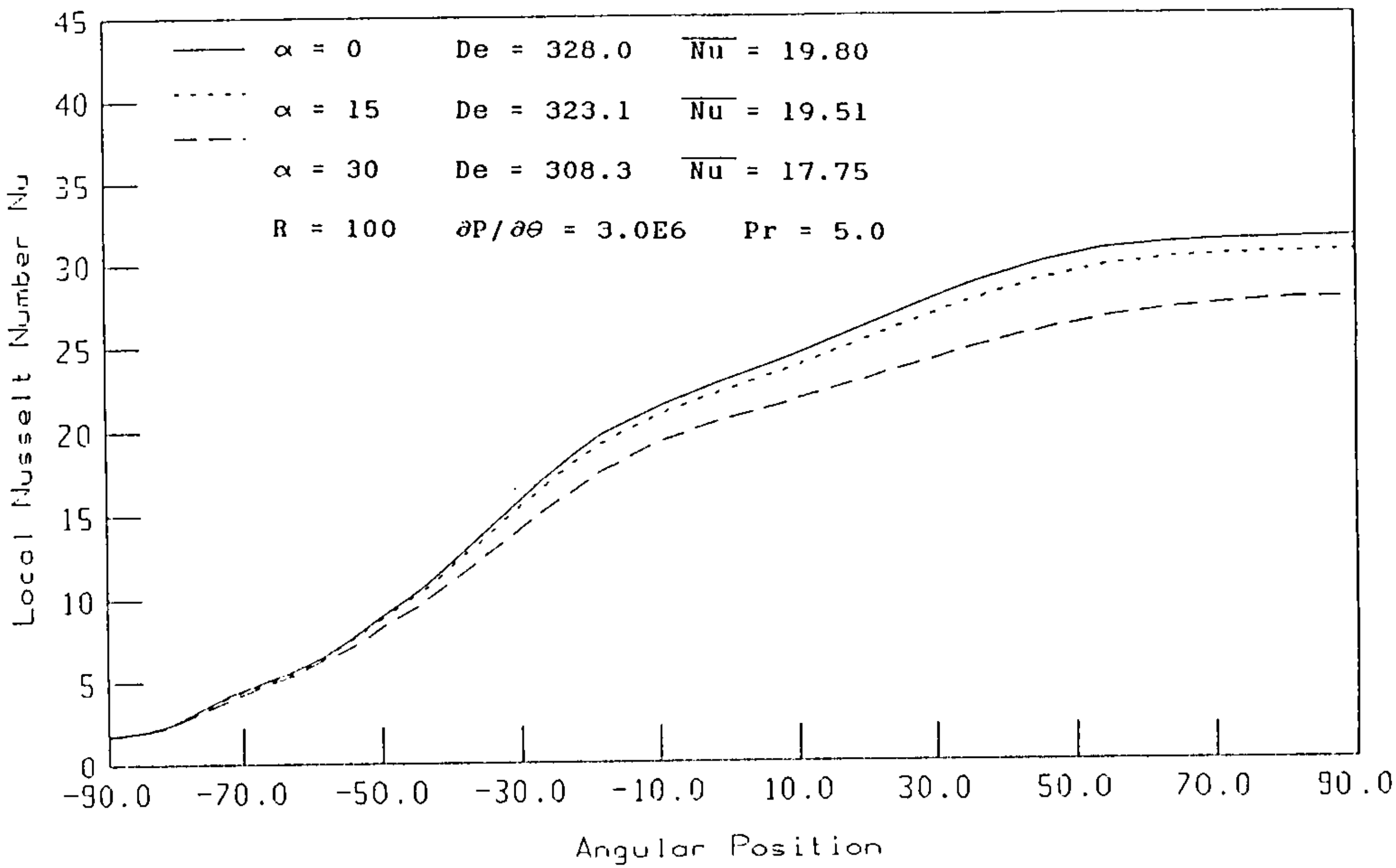


Figure (5-18) : Local Nusselt number at the wall vs angular position $\phi$

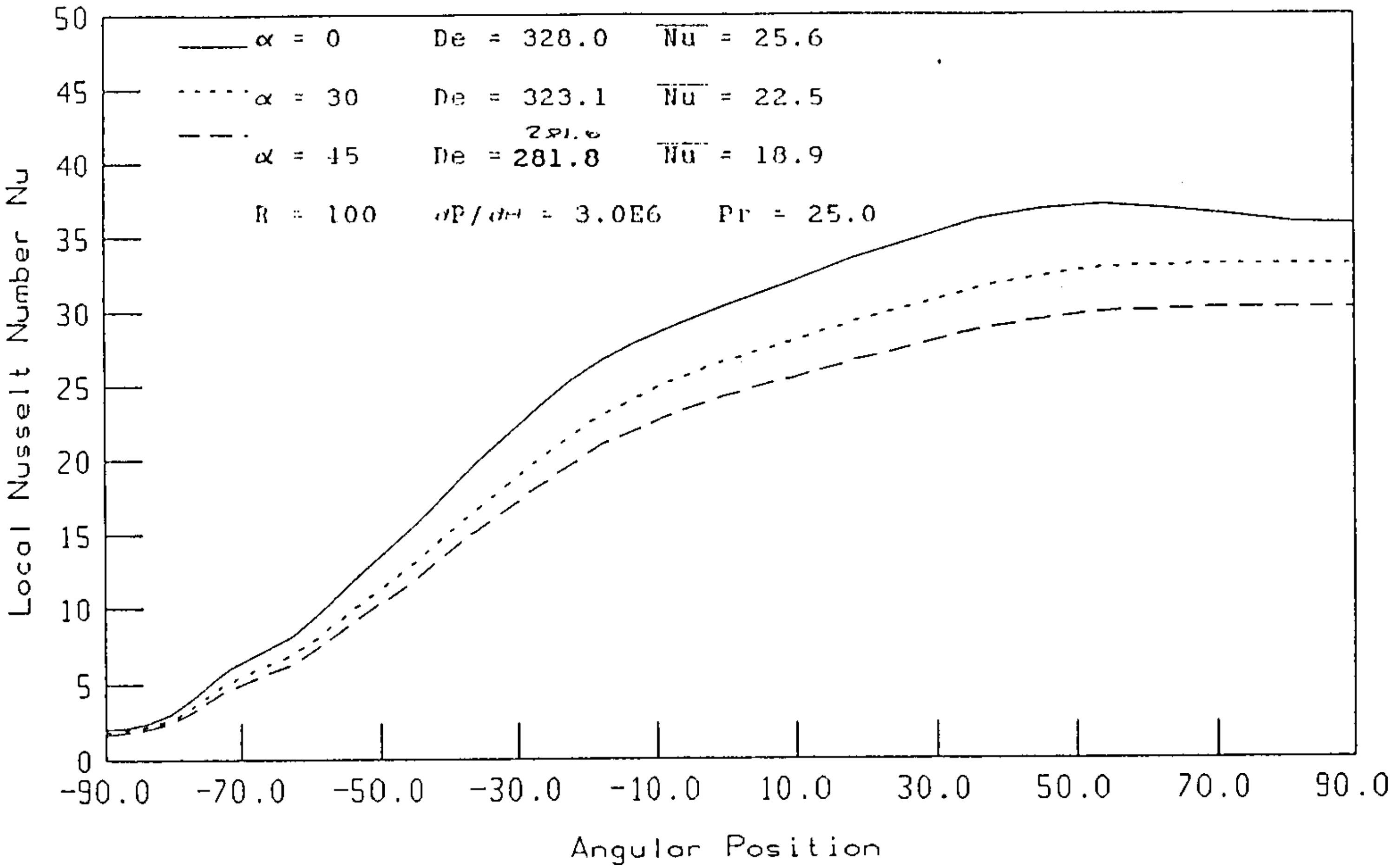


**Figure (5-19) : Local Nusselt number at the wall vs angular position $\phi$**

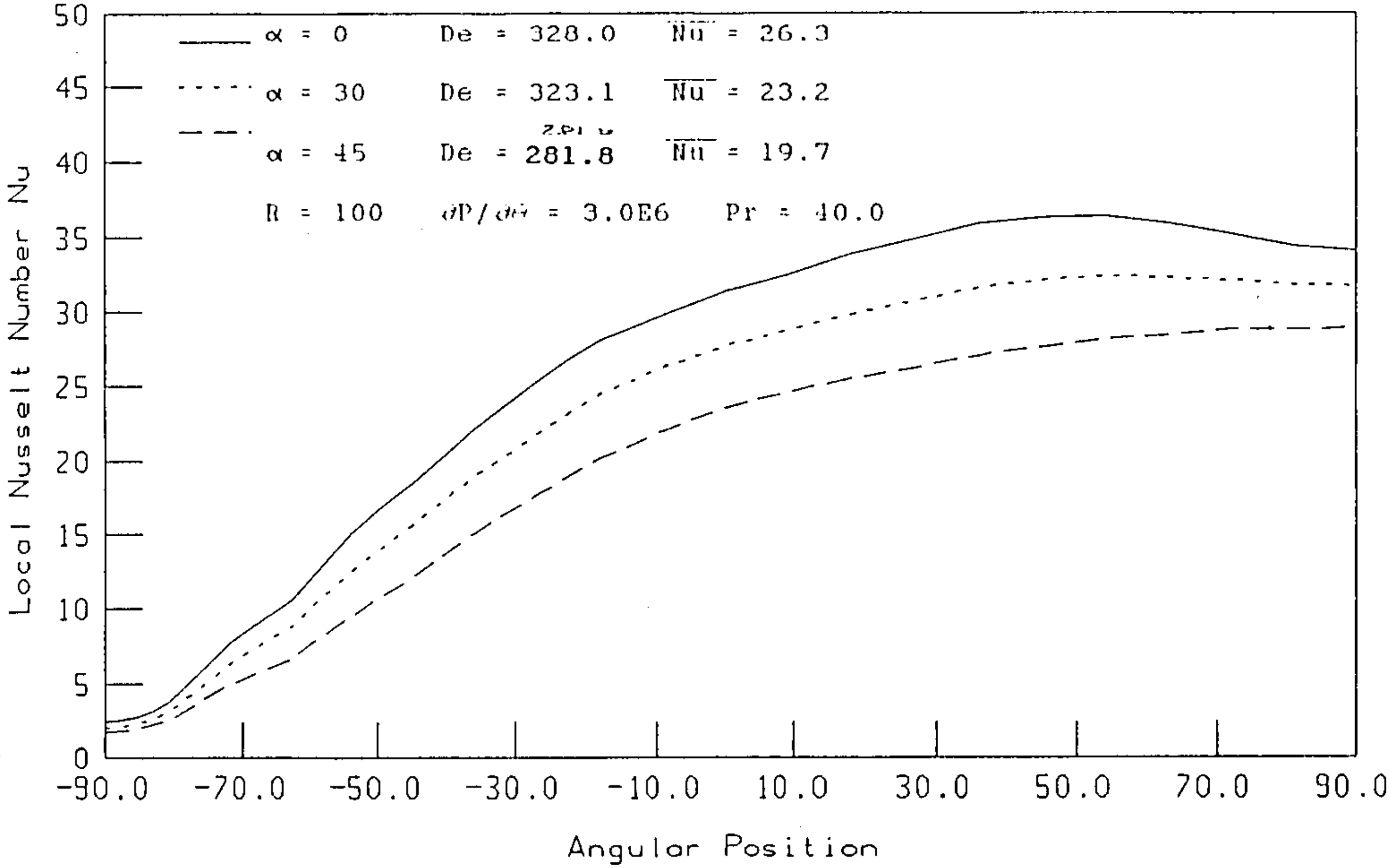


**Figure (5-20) : Local Nusselt number at the wall vs angular position $\phi$**

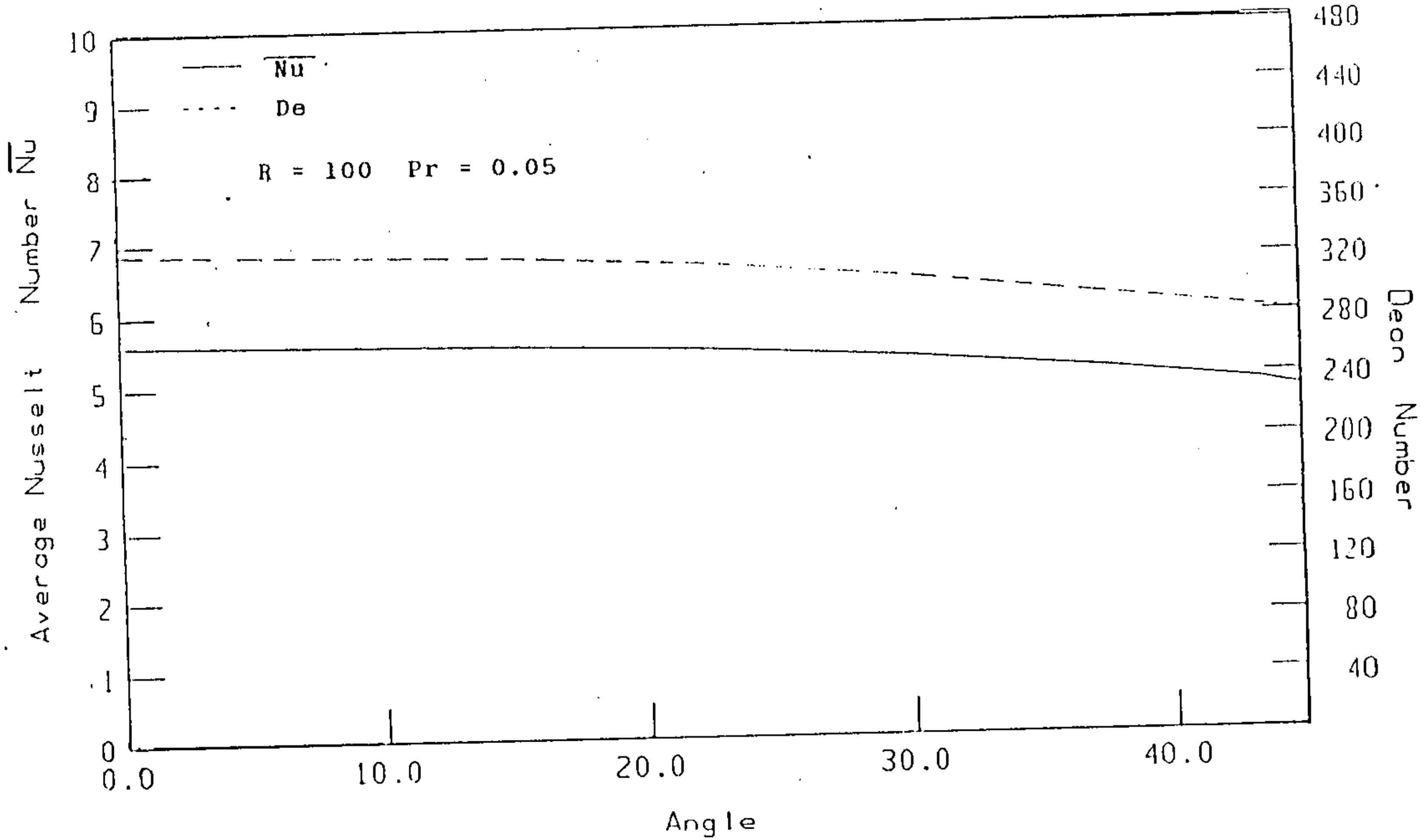


Figure (5-21) : Peripherally average Nusselt number vs tube axis inclination angle $\alpha$

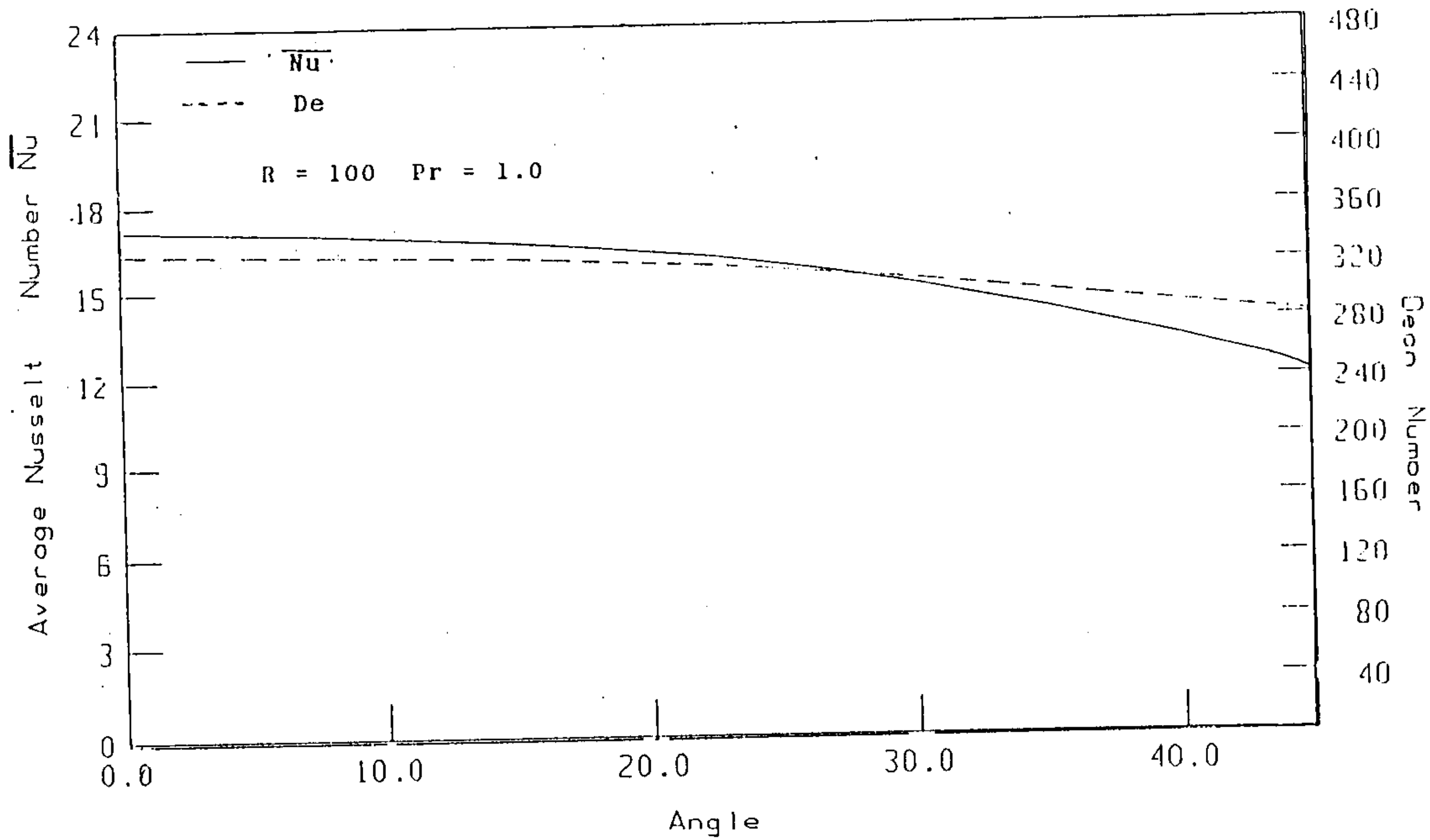


Figure (5-22) : Peripherally average Nusselt number vs tube axis inclination angle $\alpha$

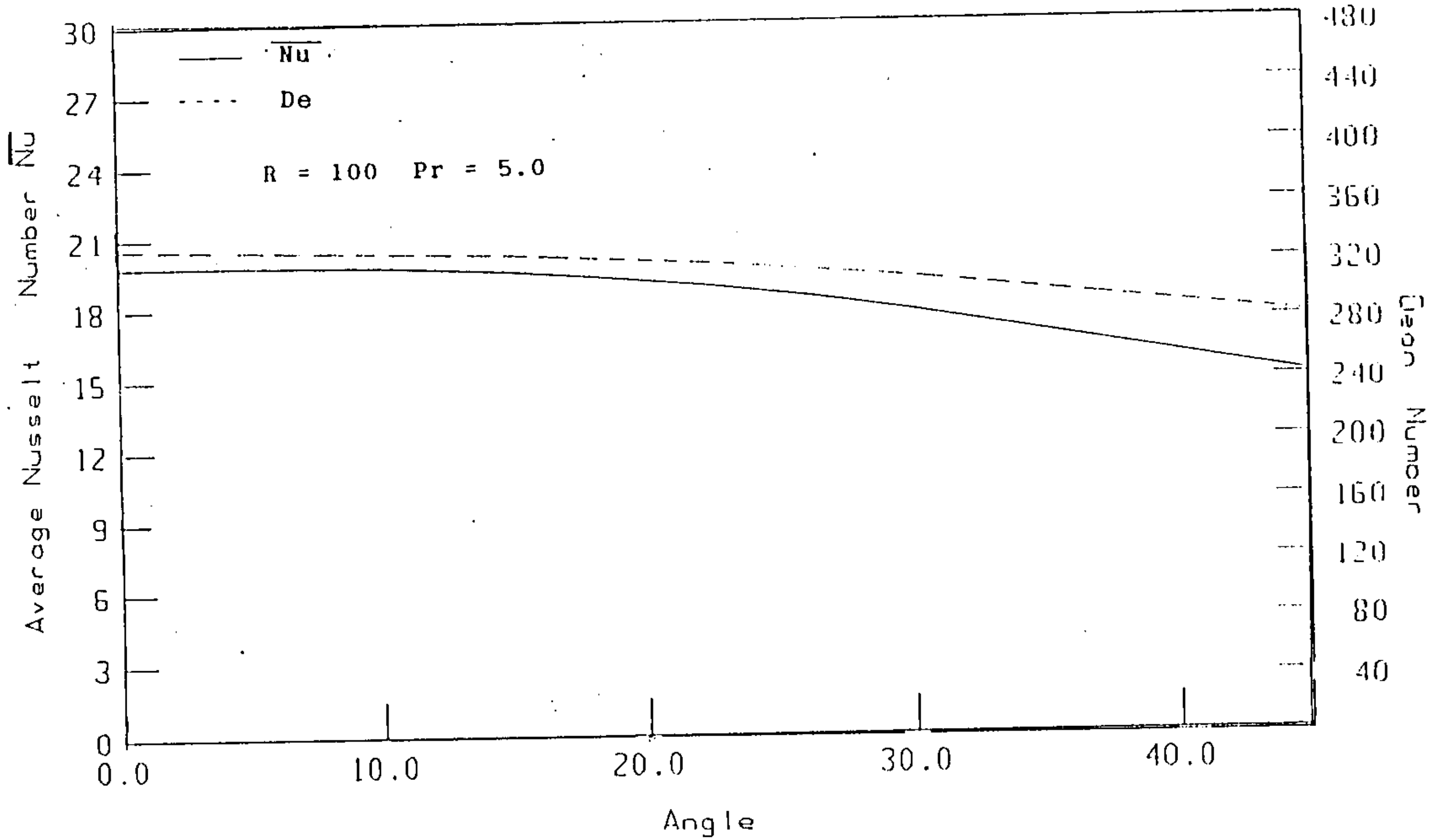


Figure (5-23) : Peripherally average Nusselt number vs tube axis inclination angle $\alpha$

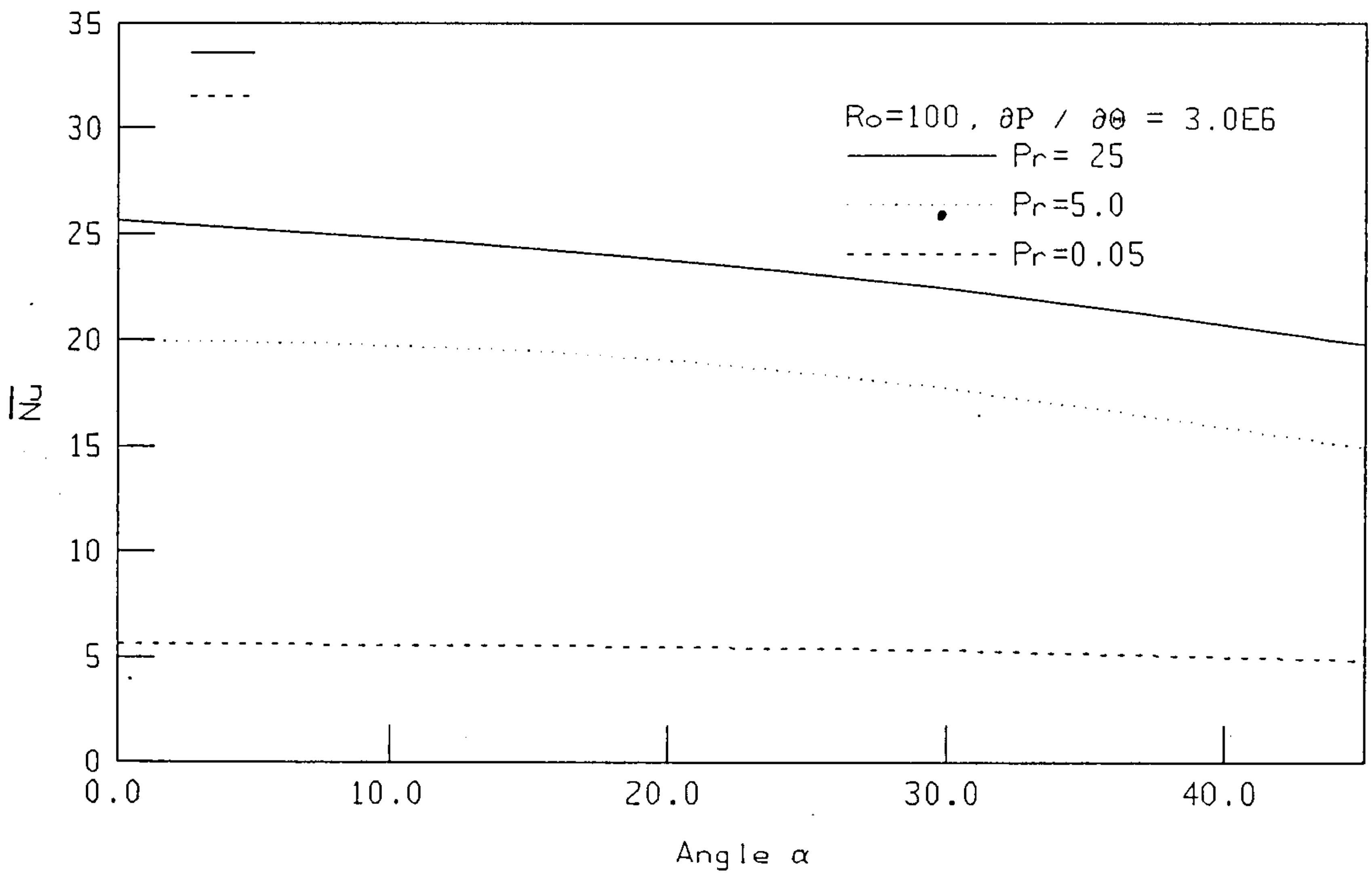


Figure (5-24) : Peripherally average Nusselt number vs tube number vs axis inclination angle α

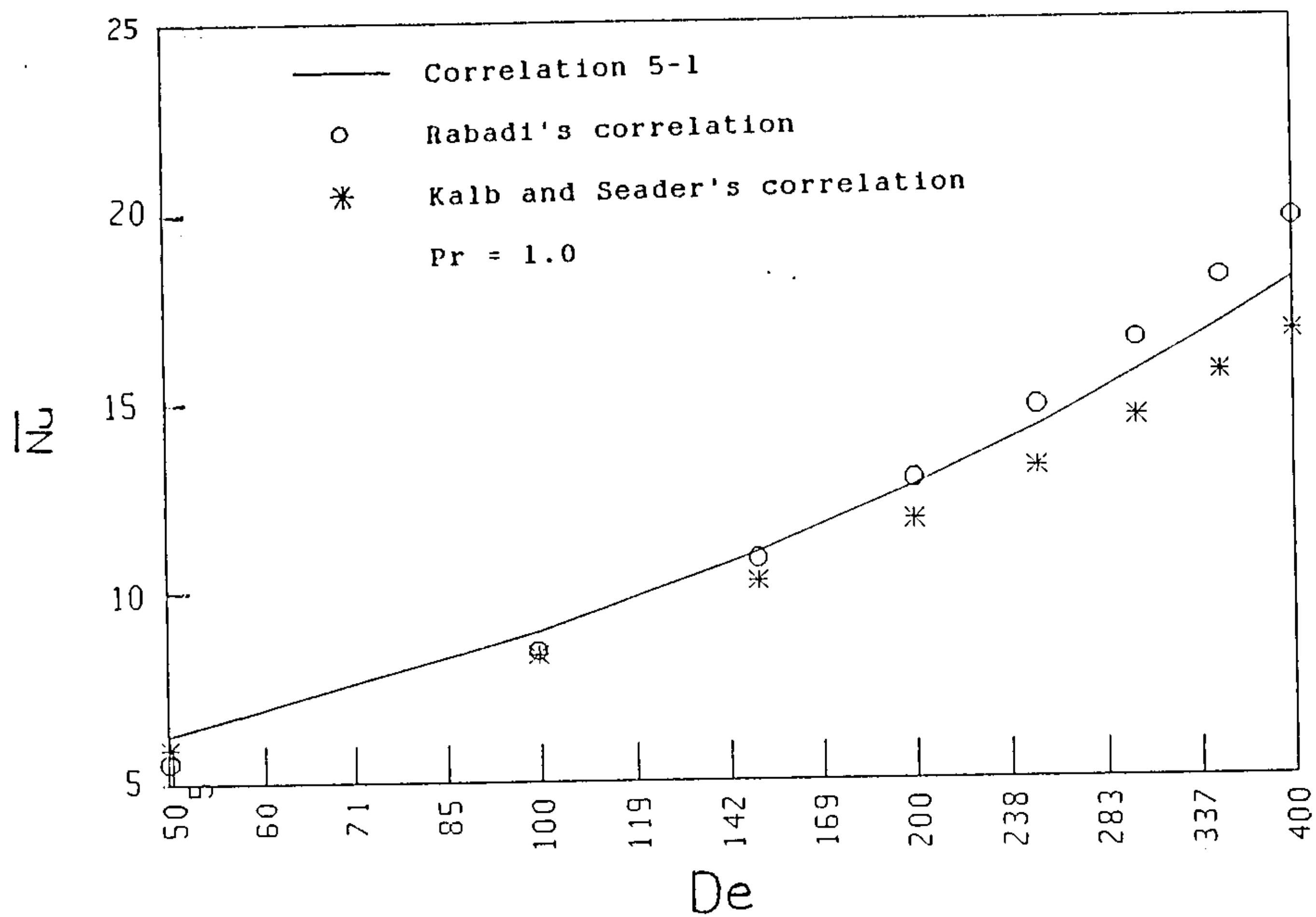


Figure (5-25) : Average Nusselt number vs Dean number

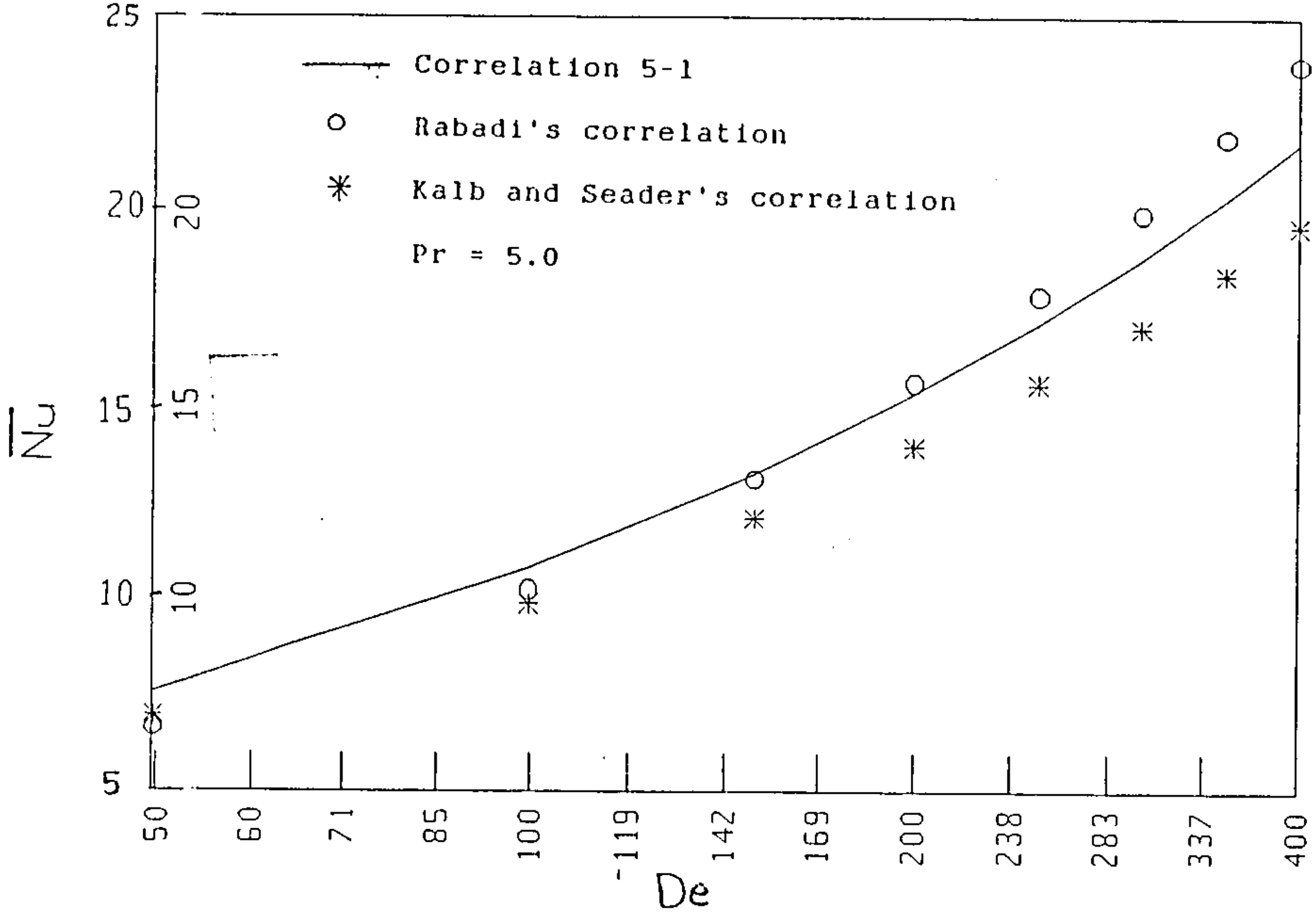


Figure (5-26) : Average Nusselt number vs Dean number

# CHAPTER 6

# CONCLUSIONS AND RECOMMENDATIONS

## 6.1 Conclusions

This study was undertaken to investigate the effect of coil pitch on the thermal performance of helical coils. It is found that the effect of increasing pitch angle $\alpha$ on average Nusselt number, $\overline{Nu}$ , keeping both, R, $\partial P/\partial \theta$ constants, depends on fluid's Prandtl number. Low, intermediate and high Pr conclusions are as follows :

1) Low Pr; increasing $\alpha$ from $0^\circ$ to $30^\circ$ decreased $\overline{Nu}$ by about 5 % . While increasing $\alpha$ to $45^\circ$ decreased $\overline{Nu}$ by about 10% .

2) Intermediate and high Pr; increasing $\alpha$ from $0^\circ$ to $30^\circ$ decreased $\overline{Nu}$ by about 10 % . While increasing $\alpha$ to $45^\circ$ decreased $\overline{Nu}$ by about 20 %

Average Nusselt number results for Prandtl numbers of 1.0 and 5.0 are correlated by the following correlation :

$$\overline{Nu} = 0.856\ De^{0.5094}\ Pr^{0.1143}$$

As can be seen $\overline{Nu}$ is a function of Pr and De which is a function of pitch angle $\alpha$.

## 6.2 Recommendations

It is recommended to study the effect of buoyancy on flow and heat transfer in helical coils.

# REFERENCES

Adler, M., "Stromung in Gerhrummten Rohern," Zeitz. fur Ang. Math. und Mech., Band 14, 257-275 (1934)

Austin, L.R., " The Development of Visccous Flow in Coil" Ph.D. Thesis, University of Utah (1971)

Bovendeerd, P.H.M, Van Steenhoven, A.A., Van De VOSSE, F.N., and Vossers, G., " Steady Entry Flow in Curved Pipe ", J. Fluid Mech. ,vol. 177, pp.233 - 246 (1987).

Chilukuri, R., and Humphrey, J.A.C., " Numerical Computation of Buoyancy-Induced Recirculation in Curved Square Duct Laminar Flow ", Int. J. Heat and Mass Transfer, vol. 24, pp 305 - 314 (1980).

Dean, W.R., 'Note on the Motion of Fluid in Curved Pipe,' Phil. Mag., vol. 4, 208-223 (1927)

Dravid, A.N., Smith, K.A., Merrill, E.W., and Brian, P.L.T. "Effect of Secondary Fluid Motion on Laminar Flow Heat Transfer in Helically Coiled Tubes ", AIChE J.,vol. 17, No. 5 PP 1114-1122 (1971)

Futagami, K., and Aoyama, Y., " Laminar Heat Transfer in a Helically Coiled Tube ", Int. J. Heat Mass Transfer,vol. 31, No. 2. pp. 387 - 396 (1988).

Hawes, W.B., " Some Sidelight on the Heat Transfer Problem," Trans. Inst Chem. Eng. 10, 162-167 (1932)

Humphrey, J.A.C., " Some Numerical Experiments on Developing Laminar Flow in Circular-Sectioned Bends ",J. Fluid Mech., vol. 154, pp. 357-375 (1985).

Janssen, L.A.M., and Hoogendoorn, C.J., "Laminar Convective Heat Transfer in Helical Coiled Tubes ", Int. J. Heat Mass Transfer, vol. 21, pp. 1197-1206 (1978).

Kalb, C.E., and Seader, J.D., " Heat and Mass Transfer Phenomena for Viscous Flow in Curved Circular Tubes ", Int. J. Heat Mass Transfer. vol, 15, pp. 801-817 (1972).

Kalb, C.E., and Seader, J.D., "Fully Developed Viscous-Flow Heat Transfer in Curved Circular Tubes with Uniform Wall Temperature ", AIChE, J.,vol. 20, No. 2 (1974).

Kalb, C.E., and Seader, J.D. " Entrance Region Heat Transfer in a Uniform wall-Temperature Helical Coil with Transition from Turbulent to Laminar Flow ", Int. J. Heat Mass Transfer, vol. 26, No. 1, pp. 23-32 (1983).

Prusa, J.and Yao, L.S., "Numerical Solution for Fully Developed Flow in Heated Curved Tubes ", J. Fluid Mech., vol. 123, pp. 503-522 (1982).

Rabadi, N.J., Chow, J.C.F., and Simon, H.A.," An Efficient Numerical Procedure for the Solution of Laminar Flow and Heat Transfer in Coiled Tubes ", Numerical Heat Transfer, vol. 2, pp. 279-289 (1979).

Rabadi, N.J.," Pulsating Flow and Heat Transfer in Curved Tubes ", Ph.D thesis, University of Illinois at Chicago Circle (1980).

Rabadi, N.J., " Heat Transfer in Curved Tubes with Pulsating Flow ", Int. J. Heat Mass Transfer, vol. 25, No. 2, pp. 195-203 (1982).

Rabadi, N.J.," Heat Transfer in Coils ", Dirasat vol. 16, No. 5 (1989).

Sumida, M., Sudou, K., and Wada, H.," Pulsating Flow in a Curved pipe ", JSME Int. J. (1989).

Truesdell, JR., and Adler, R.J., " Numerical Treatment of Fully Developed Laminar Flow in Helically Coiled Tubes ", AIChE J. (1970).

White, C.M., " Stream-Line Flow Through Curved Pipes ", Proc. roy. Soc., a123, P. 645 (1929)

Zapryanov, Z., Christove, Ch., and Toshev, E. " Fully Developed Laminar Flow and Heat Transfer in Curved Tubes ", Int. J. Heat Mass Transfer, vol. 23, pp. 873-880 (1979).

# APPENDIX A

Table (A.1): Results obtained for different pitch angels and pressure gradients for $R_o$ = 100, Pr = 0.05

| $\alpha$ | $\partial P / \partial \theta$ | De | $\overline{Nu}$ |
|---|---|---|---|
| 0 | 4.0E5 | 73.14 | 4.40 |
| 15 | = | 71.70 | 4.30 |
| 30 | = | 67.00 | 4.17 |
| 45 | = | 59.00 | 4.00 |
| | | | |
| 0 | 1.2E50 | 169.0 | 4.80 |
| 15 | = | 166.8 | 4.72 |
| 30 | = | 158.3 | 4.64 |
| | | | |
| 0 | 3.0E6 | 328.0 | 5.60 |
| 15 | = | 323.1 | 5.53 |
| 30 | = | 308.3 | 5.30 |
| 45 | = | 281.9 | 4.84 |

Table (A.2): Results obtained for different pitch angels and pressure gradients for $R_o$ = 100, Pr = 1.0

| $\alpha$ | $\partial P/\partial \theta$ | De | $\overline{Nu}$ |
|---|---|---|---|
| 0 | 4.0E5 | 73.14 | 7.66 |
| 15 | = | 71.70 | 7.50 |
| 30 | = | 67.00 | 7.00 |
| 45 | = | 59.00 | 6.20 |
| | | | |
| 0 | 1.2E50 | 169.0 | 11.6 |
| 15 | = | 166.8 | 11.3 |
| 30 | = | 158.3 | 10.4 |
| | | | |
| 0 | 3.0E6 | 328.0 | 17.2 |
| 15 | = | 323.1 | 16.7 |
| 30 | = | 308.3 | 15.2 |
| 45 | = | 281.9 | 12.2 |

Table (A.3): Results obtained for different pitch angels and pressure gradients for $R_o$ = 100, Pr = 5.0

| $\alpha$ | $\partial P/\partial\theta$ | De | $\overline{Nu}$ |
|---|---|---|---|
| 0 | 4.0E5 | 73.14 | 9.27 |
| 15 | = | 71.70 | 9.08 |
| 30 | = | 67.00 | 8.61 |
| 45 | = | 59.00 | 7.85 |
| | | | |
| 0 | 1.2E50 | 169.0 | 13.6 |
| 15 | = | 166.8 | 13.3 |
| 30 | = | 158.3 | 12.2 |
| | | | |
| 0 | 3.0E6 | 328.0 | 19.8 |
| 15 | = | 323.1 | 19.5 |
| 30 | = | 308.3 | 17.75 |
| 45 | = | 281.9 | 15.0 |

Table (A.4): Results obtained for different pitch angels and pressure gradients for $R_o$ = 100, Pr = 25.0

| $\alpha$ | $\partial P / \partial \theta$ | De | $\overline{Nu}$ |
|---|---|---|---|
| 0 | 3.0E6 | 328.0 | 25.6 |
| 30 | = | 308.3 | 22.5 |
| 45 | = | 281.8 | 18.9 |

Table (A.5): Results obtained for different pitch angels and pressure gradients for $R_o$ = 100, Pr = 40.0

| $\alpha$ | $\partial P / \partial \theta$ | De | $\overline{Nu}$ |
|---|---|---|---|
| 0 | 3.0E6 | 328.0 | 26.3 |
| 30 | = | 308.3 | 23.2 |
| 45 | = | 281.8 | 19.73 |

# FLOW CALCULATION PROGRAM

```
C         NF : Maximum number allowed for major cycle iterations.
C         PPSI : Maximum relative error allowed for the convergence on the
C                stream function.
C         PXSI : Maximum relative error allowed on the vorticity.
C         PW : Maximum relative error allowed on axial velocity.
C         PZ : Over relaxation factor used for the stream function eqation
C              solution.
C         XZB : Under relaxation factor used for the calculation of the
C               vorticity at the wall
C         RE : Reynolds number.
C         DE : Dean number.
C         TCY1 : Number of major cycle iterations.
C         CP : Pressure gradient.
C         Ro : curvature ratio.
C         W, PSI, and XI : Axial velocity stream function and vortesity.
CC
      IMPLICIT REAL *8(A-H,O-Z)
      DIMENSION  XSI(21,21),W1(21,21),XSI1(21,21),W(21,21),
     *   RD(20),YRRR(20,20),W2(21,21),
     *   PCC(20,20),PS(20),T(21),XSI2(21,21),
     *   Z1(20,20),Z2(20,20),Z3(20),Z4(20,20),Z5(20,20),
     *   Y3T(20,20),Y3R(20,20),XSIB(21),
     *  DW(20,20),TW(7,7),BW(7,7),RI(21),
     *   TXSI(7,7),BXSI(7,7),X3T(20,20),
     *   PSI(21,21),PSS(20,20),PC(21),YHH(20,20),R(21),
     *   RDJ(21),R1(20,20),H(21,21),Z(41,41),
     *   X1(20,20),X2(20,20),X4(20,20),X5(20,20),
     *   VR4(21),XR4(21),VT4(21),XT4(21),BPSI(6,6),X3R(20,20),
     *   TPSI(6,6),VR1(21),VR2(21),VR3(21),VT1(21),VT2(21),
     *   VT3(21),XT1(21),XT2(21),XT3(21),XR1(21),XR2(21),XR3(21),
     *   YH(20,20),YRR(20,20),S(21,21),PRAN(4),
     *   CTRL(20),CTTR(20),TR1(21),TR2(21),TR3(21),TT1(21),TT2(21),
     *   TT3(21),TR4(21),TT4(21),T1(21,21),TTEMP(6,6),
     *   Q1(20,20),Q2(20,20),U1(20,20),U2(20,20),
     *   FANG(21),cwt(21,21),Tmr(21),TT(21,21),
     *   Y3TX(20,20),Y3RX(20,20),X3TX(20,20),X1X(20,20),X2X(20,20),
     *   X4X(20,20),X5X(20,20),X3RX(20,20),u(21,21)
      INTEGER TOTALS,ORDER,READB,TCYL,COUNT, nheat,mread

         OPEN(4,FILE='fluid.DAT',STATUS='OLD')

         OPEN(6,FILE='fluid.OUT',STATUS='NEW')
         OPEN(7,FILE='WPLOT.OUT',STATUS='NEW')

C=====================================================================

C        INPUT DATA

C=====================================================================
         WRITE(*,*)'NHEAT='
         READ(*,*)NHEAT

         WRITE(*,*)'ALFA='
         READ(*,*)ALF

         WRITE(*,*)'RO='
         READ(*,*)RO
```

```
          NF=200
          N=21
          M3=21
          TOTALS=20
          PPSI=1.0D-5
          PW=1.0D-5
          PZ=1.7D0
          XZB=0.7D0

C------) ROH IS THE RELAXATION PARAMETER FOR XSI

C------) ROW IS THE RELAXATION PARAMETER FOR W

          ROH=20.0D0
          ROW=10.0D0
          ORDER=1
          READB=2

          TCYL=200
          NPR=1

          IWORK=0

          OPEN(UNIT=8,FILE='N.DAT',TYPE='new')
      WRITE(8,*) CP,RO,ALFHA,RAT,N,TOTALS,ORDER,PPSI,M3,NF,READB,PW,NT
     *,TCYL,PTEMP,MT,NPR,PZ,ROW,PZZ,ROH,XZB,PRAN(1),ROT1,PRAN(2),ROT2,
     *PRAN(3),ROT3,PRAN(4),ROT4
 42   FORMAT (//2(132(1H*)/)/T64,'CP= ',F11.0/T64,'RO= ',F11.2/T64,'ALPH
     *A',F11.2/T64,'RATIO=',F11.2//T16,'N =',I4,T48,'TOTALS=',I4,T80,'OR
     *DER =',I4,T112,'PPSI=',F8.6/T16,'M3=',I4,T48,'NF    =',I4,T80,'READ
     *B=',I4,T112,'PW =',F8.6/T16,'NT=',I4,T48,'TCYL =',I4,T112,'PTEMP
     * =',F8.6/T16,'MT=',I4,T48,'NPR=',I4/T5,'PZ =',F6.2,T55,'ROW =',F6.
     *2/T5,'PZZ=',F6.2,T55,'ROH =',F6.2/T5,'XZB=',F6.2,T30,'PR1=',F6.3,T
     *55,'ROT1=',F6.2/T30,'PR2 =',F6.3,T55,'ROT =',F6.2/T30,'PR3=',F6.3,
     *T55,'ROT3=',F6.2/T30,'PR4=',F6.3,T55,'ROT4=',F6.2//2(132(1H*)/))
C
CC
CC                     FORMATE STATEMENTS
CC
    7 FORMAT(1X,'AWW=',F9.6,2X,'AX=',F9.6,2X,'W(2,1)=',d20.10,2X,'XSI(1
     *,N1)=',d20.10/)
    9 FORMAT(5X,'LT=',I4/)
 53   FORMAT(10X,'ifail= ',I3,5X,'T. O. C. DUE TO SIGULARITY -1-')
 59   FORMAT(10X,'ifail= ',I3,5X,'T. O. C. DUE TO SIGULARITY -3-')
 56   FORMAT(10X,'ifail= ',I3,5X,'T. O. C. DUE TO SIGULARITY -2-')
 55   FORMAT(10X,'ifail= ',I3,5X,'T. O. C. DUE TO SIGULARITY -4-')
 63   FORMAT(10X,'ifail= ',I3,5X,'T. O. C. DUE TO SIGULARITY -5-')
 66   FORMAT(2X,' TERMINATION OF CALCULATION IS DUE TO STREAM FUNCTION
     * FAILING TO CONVERGE ')
 140  FORMAT(6d20.11/6d20.11/6d20.11/3d20.11/)
 142  FORMAT (30X,'AXIAL VELOCITY'///)
 141  FORMAT(30X,'STREAM FUNCTION'///)
 143  FORMAT(30X,'  VORTICITY     '///)
 144  FORMAT(20X,'MS=',I4,5X,'AP=',F9.6/)
 300  FORMAT(4D20.11/4D20.11/4D20.11/4D20.11/4D20.11/1D20.11)
 997  FORMAT(///10X,'G R E A T ,{{  CONGRATULATIONS  }} '//)
CC                     GRID POINTS SPACE ASSIGNMENTS
cc
cc        CWTF IS RELAXATION FACTOR
cc
```

```
          cwtf = 1.0
cc
cc
cc
cc              m3 is the number of divisions along the radius
cc              n  is the number of divisions along the circmference
CC
      NN=N-1
      N1 = NN/2 +1
      M4 =M3-1
      DR=1.0D0/M4
      PIE=3.141592653589BD0
      DPHI=PIE/NN
      PHI=1.0D0/DPHI
      PH=PHI/DPHI
      DO 31 J=1,M3
   31 R(J) =1.0D0-(J-1)*DR
      DRA=1.0D0/DR
      DRA2 = 2.0D0*DRA*DRA
      DRH=DR/DPHI
      R(M3) = 0.0D0
      RDJ(M3)=0.0D0
c
      DO 50 J=1,M4
      RDJ(J)=R(J)*R(J)
      RD(J)=   RDJ(J)*DRA/2.0D0
c
      DO 50 K=1,NN
      T(K)=-0.5D0*PIE+(K-1)*DPHI
      R1(J,K)=R0+R(J)*DSIN(T(K))
      YH(J,K)=1.0D0/R1(J,K)/R1(J,K)
      YHH(J,K)=1.0D0/R(J)/R1(J,K)
      YRR(J,K)=DR*R1(J,K)
      YRRR(J,K)=DR*YRR(J,K)
      PC(K)=DSIN(T(K))/2.0D0/DR
      PCC(J,K)=R(J)*DCOS(T(K))/2.0D0/R1(J,K)
      PS(K)=DSIN(T(K))/2.0D0/DPHI
   50 PSS(J,K)=DSIN(T(K))/2.0D0/R1(J,K)
c
      T(1)  = -PIE/2.0D0
      T(21) = PIE/2.0D0
      PC(1) = 0.0D0
      PC(N) = 0.0D0
      PS(N1)= 0.0D0
c
      DO 150 J =1,M4
      PCC(J,1) =0.0D0
  150 PSS(J,N1)=0.0D0
CC
CC                        PREPARATION FOR ITERATION
CC
      DO 6 J=1,M4
      Z3(J) =-2.0D0*(2.0D0*RD(J)+DR*PH)
c
      DO 6 K =1,NN
      Z2(J,K)=(DRH     )*(PCC(J,K)+PHI)
      Z4(J,K)=(DRH )*(-PCC(J,K)+PHI)
      Z1(J,K)=RDJ(J)    *( 0.5D0/R(J)+DRA -PSS(J,K))
```

```
    6  Z5(J,K)=RDJ(J)    *(-0.5D0/R(J)+DRA +PSS(J,K))
C-----------------------------------------------------------------
C%%%%%%   INITIAL FIELD
C-----------------------------------------------------------------

      IF(readB.NE.1) GO TO 2
c
      DO 4    J=1,M3
      DO 4    K=1,N
C                XSI(J,K)=0.0D0
      PSI(J,K)=0.0D0
    4 W(J,K)   =  CP*(1.0D0-RDJ(J))/R0/4.0D0
c
C           WRITE(8,300) ((W(J,K),K=1,N),J=1,M3)

      GO TO 5

    2       DO 604,K=1,21
            DO 604,J=1,21
  604       read(4,*)w(j,k),xsi(j,k),psi(j,k)


C           WRITE(*,*)COS(ALF)
CC                           NON-LINEAR COEFFICIENTS
    5 CONTINUE
CC
      DO 13 J=2,M4
      DO 13 K=2,NN
CC
      ASI=YH(J,K)*(1.-(PC(K)/COSD(ALF)*(PSI(J-1,K)-PSI(J+1,K)))
     *   +(PS(K)/COSD(ALF)/R(J))*
     *    (PSI(J,K+1)-PSI(J,K-1)))


      B=YHH(J,K)/COSD(ALF)*(PSI(J-1,K)-PSI(J+1,K))/2./COSD(ALF)
     *   /DR-2.*DR*PC(K)*YHH(J,K)/COSD(ALF)


      C=-(1./COSD(ALF)/R(J)+2.0*PSS(J,K)+(YHH(J,K))/COSD(ALF)*
     *   (PSI(J,K+1)-PSI(J,K-1))/2
     *  .0/DPHI)



CC
             A=0.0
      X1(J,K)=DRA*(C/2.0D0-DRA)

      X2(J,K)=PHI*(-B*/2.0D0-PHI/RDJ(J))

      X3R(J,K)  =  DRA2

      X3T(J,K)  =  2.0D0*PH/RDJ(J)

      Y3R(J,K)  =  DRA2

      Y3T(J,K)  =  2.0D0*PH/RDJ(J)

      X4(J,K)=PHI*(B/2.0D0-PHI/RDJ(J))
```

```
      X5(J,K)=DRA*(-C/2.0D0-DRA)

         X1X(J,K)=X1(J,K)
         X2X(J,K)=X2(J,K)
         X3RX(J,K)=X3R(J,K)
         X3TX(J,K)=X3T(J,K)
         Y3RX(J,K)=Y3R(J,K)
         Y3TX(J,K)=Y3T(J,K)
         X4X(J,K)=X4(J,K)
         X5X(J,K)=X5(J,K)

   13 CONTINUE
CC

C
      DO 107 J=1,M3
      DO 107 K=1,N
      W1(J,K)=0.0D0
      W2(J,K)=0.0D0
      XSI1(J,K)=0.0D0
  107 XSI2(J,K)=XSI(J,K)
C SSSSSSSSSSSSSSSSSSSSSSSSSSSSSSSSSSSSSSSSSSSSSSSSSSSSSSSSSSSSSSSSSSSS
      DO 320 K=1,N
  320 XSIB(K)=XSI(1,K)
C SSSSSSSSSSSSSSSSSSSSSSSSSSSSSSSSSSSSSSSSSSSSSSSSSSSSSSSSSSSSSSSSSSSSS
CC


      DO 1 LT= 1,NF
      WRITE(8,9) LT
      IJ=-1
      DO 129  J=1,7
      IJ=IJ+3
      IK=-2
      DO 129 K=1,7
      IK=IK+3
      TXSI(J,K)=DABS(XSI(IJ,IK))
  129 TW(J,K)=DABS(W(IJ,IK))
CC
CC
CC
      VR22 =(X3R(N1,N1))*ROW
      DO 17 I= 2,M4
      VR1(I) = X1(I,N1)
      VR2(I) =X3R(I,N1)+VR22
      VR3(I+1) = X5(I,N1)
      VR4(I)=(CP*COSD(ALF)/R1(I,N1)-(X2(I,N1)*W(I,N1-1)+X4(I,N1)*W(I,N1+1
     /         X3T(I,N1))*W(I,N1)+VR22*W(I,N1)+Ueff(j,k)
  17  CONTINUE
CC                 B.C. AT THE WALL
      VR2(1) =1.0+VR22
      VR3(2) = 0.0
      VR4(1) = 0.0
      VR1(1) = 0.0
CC
CC                 B.C. AT THE CENTER
      VR2(M3) = 1.0+VR22
      VR1(M3) =-1.0
```

```
      VR4(M3) = 0.333*(W(M4,N1)-W(M3-2,N1))+VR22*W(M3,N1)
c         VR4(M3)=0.5*(W(M4,N1)-W(M3,N1))+VR22*W(M3,N1)
          CALL F04EAF(21,VR2,VR3,VR1,VR4,IFAIL)
      IF(ifail.NE.0) GO TO 52
CC
      W(M3,N1)=VR4(M3)
CC
C ########################################################################
C ########################################################################
CC
          vr22=(x3r(n1,n1))*row
cc
      DO 3 K=2,NN
      DO 25 I=2,M4
      VR1(I) = X1(I,K)
      VR2(I) =X3R(I,K)+VR22
      VR3(I+1) = X5(I,K)
   25 VR4(I)=(CP*COSD(ALF)/R1(I,K)-(X2(I,K)*W(I,K-1)+X4(I,K)*W(I,K+1)))-(
     /          X3T(I,K))*W(I,K)+VR22*W(I,K)
CC
CC                     B.C. AT THE WALL
      VR1(1) = 0.0D0
      VR3(2) = 0.0D0
      VR2(1) = 1.0D0+VR22
      VR4(1) = 0.0D0
CC
CC                     B.C. AT THE CENTER
      VR2(M3) = 1.0D0+VR22
      VR1(M3) = 0.0D0
      VR4(M3) = W(M3,N1)+VR22*W(M3,N1)
CC
        CALL F04EAF(21,VR2,VR3,VR1,VR4,IFAIL)
      IF(ifail.NE.0) GO TO 57
      DO 169 I=2,M3
  169 W1 (I,K)=VR4(I)
c
    3 CONTINUE
c
      DO 117 J=2,M4
      W1(J,1) = (4.0D0*W1(J,2)-W1(J,3))/3.0D0
  117 W1(J,N) = (4.0D0*W1(J,NN)-W1(J,NN-1))/3.0D0
c
      W1(M3,1)=W1(M3,N1)
      W1(M3,N)=W1(M3,N1)
CC
      VT22=(X3T(N1,N1))*ROW
C
      DO 21 J=2,M4
      DO 18 I= 2,NN
CC
      VT1(I) = X2(J,I)
      VT2(I) =X3T(J,I)+VT22
      VT3(I+1) =X4(J,I)
   18 VT4(I)=(CP*COSD(ALF)/R1(J,I)-(X5(J,I)*W1(J+1,I)+X1(J,I)*W1(J-1,I)))-(
     /          (J,I))*W1(J,I)+VT22*W1(J,I)+Ueff(j,k)
CC
CC                     B.C. AT THE L.C.L.
      VT1(1) = 0.0D0
      VT3(2) =-1.0D0
      VT2(1) = 1.0D0+VT22
```

```
      VT4(1) =0.33*(W1(J,2)-W1(J,3))+VT22*W1(J,1)
CC
CC                   B.C. AT THE R.C.L.
      VT2(N) = 1.0D0+VT22
      VT1(N) =-1.0D0
      VT4(N) =0.33D0*(W1(J,NN)-W1(J,NN-1))+VT22*W1(J,N)
CC
        CALL F04EAF(21,VT2,VT3,VT1,VT4,IFAIL)
      IF(ifail.NE.0) GO TO 61
CC
CC
      DO 19 I=1,N
 19   W2(J,I)=VT4(I)
C
 21   CONTINUE
c
      W2(M3,N1)= W2(M4,N1) + 1.0D0/3.0D0*(W2(M4,N1)-W2(M4-1,N1))
c
      DO 122 K =1,N
 122  W2(M3,K) = W2(M3,N1)
CC
CC
C $$$$$$$$$$$$$$$$$$$$$$$$$$$$$$$$$$$$$$$$$$$$$$$$$$$$$$$$$$$$$$$$$$$$$$$

CC--------------------------------------------------------------------
C                    START OF XSI (i+1/2) in r-D
C---------------------------------------------------------------------

      XR22=(Y3R(N1,N1))*RCH
c
      DO 103 K=2,NN
      DO 125 I=2,M4
      DW(I,K)=(W(I,K)+W1(I,K))*COSD(ALF)**2/R1(I,K)*(PC(K)*COSD(ALF)**2
     *          /2.0*(W(I-1,K)
     *          + W1(I-1,K)
     *           -W(I+1,K)-W1(I+1,K))-PS(K)*COSD(ALF)**2/R(I)/2.0*(W(I,K+1)
     *          +W1(I,K+1)
     *           -W(I,K-1)-W1(I,K-1)))
      XR1(I)=X1X(I,K)
      XR2(I)=Y3RX(I,K)+XR22
      XR3(I+1)=X5X(I,K)
  125 XR4(I)=(DW(I,K)-(X2X(I,K)*XSI(I,K-1)+X4X(I,K)*XSI(I,K+1)))-
     /          (Y3TX(I,K))*XSI(I,K)+XR22*XSI(I,K)
CC
      XR1(1) = 0.0D0
      XR2(1) = 1.0D0+XR22
      XR3(2) = 0.0D0
         XR4(1)=XSI(1,K)+XR22*XSI(1,K)
c        IF (lt.NE.1) XR4(1)=XSI(1,K)*(1.0D0-XZB)+XZB*XSIB(K)
      if(lt.ne.1) XR4(1)=XSI(1,K)*xzb+(1.0-xzb)*XSIB(K)+XR22*XSI(1,K)
CCCCCCXR4(1)=XSI2(1,K)+XR22*XSI(1,K)CCCCCCCCCCCCCCCCCCCCCCCCCCCCCCCCCCCC
      XR1(M3) = 0.0D0
      XR2(M3) =1.0D0+XR22
      XR4(M3) = 0.0D0
CC
        CALL F04EAF (21,XR2,XR3,XR1,XR4,IFAIL)
      IF(ifail.NE.0) GO TO 54
CC
      DO 116 I=1,M4
  116 XSI1(I,K)=XR4(I)
```

```
C
 103  CONTINUE
C
      DO 321 K=1,N
  321 XSIB(K)=XSI1(1,K)
C
C-----------------------------------------------------------------------
CC                     START OF XSI (i+1) in PHI-D
C-----------------------------------------------------------------------


      XT22=(Y3T(N1,N1))*ROH
C
C
      DO 121 J=2,M4
      DO 128 I=2,NN
      DW(J,I)=(W2(J,I)+W1(J,I))*COSD(ALF)**2/R1(J,I)*(PC(I)*COSD(ALF)**2
     *      /2.0*(W2(J-1,I)
     *      +W1(J-1,
     *       I)-W2(J+1,I)-W1(J+1,I))-PS(I)*COSD(ALF)**2/R(J)/2.0*(W2(J,I+1)
     *      +W1(J,I+1
     *         )-W2(J,I-1)-W1(J,I-1)))
      XT1(I)=X2X(J,I)
      XT2(I)=Y3TX(J,I)+XT22
      XT3(I+1)=X4X(J,I)
  128 XT4(I)=(DW(J,I)-(X5X(J,I)*XSI1(J+1,I)+X1X(J,I)*XSI1(J-1,I)))-
     &   (Y3RX(J,I))*XSI1(J,I)+XT22*XSI1(J,I)
CC
CC                       B.C. AT THE C.L.
CC
      XT1(1) = 0.0D0
      XT3(2) = 0.0D0
      XT2(1) = 1.0D0+XT22
      XT4(1) = 0.0D0
CC
CC                       B.C. AT THE C.L.
      XT2(N) = 1.0D0+XT22
      XT1(N) = 0.0D0
      XT4(N) = 0.0D0
CC
        CALL F04EAF(21,XT2,XT3,XT1,XT4,IFAIL)
      IF(ifail.NE.0) GO TO 58
CC
      DO 119 I=2,NN
  119 XSI2(J,I)=XT4(I)
C
C
 121  CONTINUE
C                        UP-DATING PSI
CC
      DO 26 MS=1,TOTALS
CC
      IJ=-1
C
      DO 29  J=1,6
      IJ=IJ+3
      IK=-1
C
      DO 29 K=1,6
      IK=IK+3
```

```
   29 TPSI(J,K)=DABS(PSI(IJ,IK))
CC
      DO 8  J=2,M4
      DO 8  K=2,NN
      XSR=DR
    8 PSI(J,K)=(XSR-Z1(J,K)*PSI(J-1,K)-Z2(J,K)*PSI(J,K-1)-Z4(J,K)*PSI(J,
     *K+1)-Z5(J,K)*PSI(J+1,K))/Z3(J)*PZ+(1.0D0-PZ)*PSI(J,K)
CC
      AP=0.0D0
      IJ=-1
       DO 11  J=1,6
      IJ=IJ+3
      IK=-1
C
       DO 11 K=1,6
       IK=IK+3
      BPSI(J,K) =DABS(PSI(IJ,IK))
C         IF(BPSI(J,K) .LT. 100.0D0) GO TO 11
      APSI=DABS((BPSI(J,K)-TPSI(J,K))/BPSI(J,K))
      IF(APSI.LE.AP) GO TO 11
      AP=APSI
      IF (AP.GT.1.AND.MS.GT.TOTALS) GO TO 65
   11 CONTINUE
C
      IF(AP  .LT.PPSI)        GO TO 733
 26   CONTINUE
C
  733 GO TO (744,745,747),ORDER
  744 DO 734 K=2,NN
  734 XSI2(1,K)=((4.0D0*PSI(2,K)-0.5D0*PSI(3,K))/(DR)**2)*XZB+
     *      (1.0D0-XZB)*XSI2(1,K)
      GO TO 738
  745 DO 735 K=2,NN
  735 XSI2(1,K)=(2.0D0*PSI(2,K)/(DR)**2)*XZB+(1.0-XZB)*XSI2(1,K)
      GO TO 738
  747 DO 737 K=2,NN
  737 XSI2(1,K) =((6.0D0*PSI(2,K)-1.50*PSI(3,K)+2.0/9.0*PSI(4,K))/
     /                (DR)**2)*XZB+(1.0-XZB)*XSI2(1,K)
  738 CONTINUE




CC
CC                      NON-LINEAR COEFFICIENTS
CC
      DO 16 J=2,M4
      DO 16 K=2,NN

      ASI=YH(J,K)*(1.-(PC(K)/COSD(ALF)*(PSI(J-1,K)-PSI(J+1,K)))
     *    +(PS(K)/COSD(ALF)/R(J))*
     *     (PSI(J,K+1)-PSI(J,K-1)))


      B=YHH(J,K)/COSD(ALF)*(PSI(J-1,K)-PSI(J+1,K))/2./COSD(ALF)
     *    /DR-2.*DR*PC(K)*YHH(J,K)/COSD(ALF)
```

```
      C=-(1./COSD(ALF)/R(J)+2.0*PSS(J,K)+(YHH(J,K))/COSD(ALF)*
     *    (PSI(J,K+1)-PSI(J,K-1))/2
     *   .0/DPHI)


      A=YH(J,K)  *(1.+PC(K)/COSD(ALF)*(PSI(J-1,K)-PSI(J+1,K))
     *    -PS(K)/COSD(ALF)/R(J)*(PSI(
     *   J,K+1)-PSI(J,K-1)))
CC
      X1(J,K)=DRA*(C/2.0D0-DRA/COSD(ALF))

      X2(J,K)=PHI*(-B*COSD(ALF)/2.0D0-PHI/RDJ(J)/COSD(ALF))

      X3R(J,K)  =  A*COSD(ALF)/2.0D0  +DRA2/COSD(ALF)

      X3T(J,K)  =  A*COSD(ALF)/2.0D0  +2.0D0*PH/RDJ(J)/COSD(ALF)

      Y3R(J,K)  =  ASI*COSD(ALF)/2.0D0  +DRA2/COSD(ALF)

      Y3T(J,K)  =  ASI*COSD(ALF)/2.0D0  +2.0D0*PH/RDJ(J)/COSD(ALF)

      X4(J,K)=PHI*(B*COSD(ALF)/2.0D0-PHI/RDJ(J)/COSD(ALF))

      X5(J,K)=DRA*(-C/2.0D0-DRA/COSD(ALF))


         X1X(J,K)=X1(J,K)/COSD(ALF)
         X2X(J,K)=X2(J,K)/COSD(ALF)
         X3RX(J,K)=X3R(J,K)/COSD(ALF)
         X3TX(J,K)=X3T(J,K)/COSD(ALF)
         Y3RX(J,K)=Y3R(J,K)/COSD(ALF)
         Y3TX(J,K)=Y3T(J,K)/COSD(ALF)
         X4X(J,K)=X4(J,K)/COSD(ALF)
         X5X(J,K)=X5(J,K)/COSD(ALF)



  16  CONTINUE


CC
      WRITE(8,144) MS,AP
C ########################################################################
CC
CC
       DO 131 J=1,M3
       DO 131 K=1,N
      W(J,K)= W2(J,K)
  131 XSI(J,K)  =  XSI2(J,K)
C
      AX=0.0D0
      AWW=0.0D0
      IJ=-1
C
       DO 111  J=1,7
       IJ=IJ+3
       IK=-2
C
       DO 111 K=1,7
```

```
      IK=IK+3
      BW(J,K)=DABS(W(IJ,IK))
      AW=DABS((BW(J,K)-TW(J,K))/BW(J,K))
      IF(AW.LE.AWW) GO TO 101
      AWW=AW
  101 BXSI(J,K) =DABS(XSI(IJ,IK))
      IF(BXSI(J,K) .LT. 1.0D0) GO TO 111
      AXSI=DABS((BXSI(J,K)-TXSI(J,K))/BXSI(J,K))
      IF(AXSI.LE.AX) GO TO 111
      AX=AXSI
  111 CONTINUE
C
      WRITE(8,7) AWW,AX,W(2,1),XSI(1,N1)
      IF(AWW .LT. PW. AND .MS. LE .5) GO TO 998
    1 CONTINUE

          do 816 j1=2,20
          do 816 k1=2,20
 816      write(77,*) U(j1,k1)


C
 998  WRITE(8,997)
c ================= print flow field on fluid.dat ============

          do 807,k=1,21
          do 807,j=1,21
 807      write(6,*)w(j,k),',',xsi(j,k),',',psi(j,k)

c===========================================================

c******* ********  prepare axial velocity for plotting *********

c*****************************************************************

c         at   H C-L  ( LEFT )

          DELr=1.0D0/20
          WRITE(7,*) 2*M4+1
          DO 551,J=1,20
 551      WRITE(7,*)-(1.0-(J-1)*DELr),',',W(J,1)


C         AT THE CENTER POINT


          WRITE(7,*)0,',',W(21,1)

C         AT R C-L (RIGHT)

          DO 552,J=20,1,-1
 552      WRITE(7,*)1.0-(J-1)*DELr,',',W(J,21)

C===============================================================

CC   ************** CALCULATION OF REYNOLD AND DEANS NUMBERS **********
          DO 109 K=1,21
          F4=0.0
          F2=0.0
          DO 209 J=2,20,2
```

```
      F4=F4 + W(J,K)*R(J)
 209      F2=F2 + W(J+1,K)*R(J+1)
 109      RI(K)= DR*(4.0*F4 + 2.0*F2)/3.0
          F4 =0.0
          F2 =0.0
          DO 319 K=2,20,2
 319      F4 = F4 +RI(K)
          DO 139 K=3,19,2
 139      F2 = F2 +RI(K)
CC
      RE = 4.0*DPHI*(RI(1)+4.0*F4+2.0*F2+RI(M3))/(3.0*PIE)
CC
      DE = RE*COSD(ALF)/DSQRT(RO)

c-----------------------------------------------------------------------
c-----------------------------------------------------------------------

          write(7,*)'DE=',DE,'  RE=',RE

c-----------------------------------------------------------------------
      GO TO 999
  52  WRITE(8,53) ifail
      GO TO 999
  54  WRITE(8,55) ifail
      GO TO 999
  57  WRITE(8,56) ifail
      GO TO 999
  58  WRITE(8,59) ifail
      GO TO 999
  61  WRITE(8,63) ifail
      GO TO 999
 65   WRITE(8,66)
      GO TO 999

 999  CONTINUE
CC  *************** CALCULATION OF REYNOLD AND DEANS NUMBERS ***********
      DO 10 K=1,21
      F4=0.0
      F2=0.0
      DO 20 J=2,20,2
      F4=F4 + W(J,K)*R(J)
  20  F2=F2 + W(J+1,K)*R(J+1)
  10  RI(K)= DR*(4.0*F4 + 2.0*F2)/3.0
      F4 =0.0
      F2 =0.0
      DO 311 K=2,20,2
  311 F4 = F4 +RI(K)
      DO 113 K=3,19,2
  113 F2 = F2 +RI(K)
CC
      RE = 4.0*DPHI*(RI(1)+4.0*F4+2.0*F2+RI(M3))/(3.0*PIE)
CC
      DE = RE*COSD(ALF)/DSQRT(RO)
CC
          WRITE(8,30) RE,DE
   30 FORMAT(//20X,'REYNOLD NO. IS =',F9.2,5X,'DEANS NO. IS=',F9.2//)
C         ----------------------------------------------------
          STOP
          END
```

# HEAT TRANSFER CALCULATION PROGRAM

```
      DOUBLE PRECISION WO(21,21),W(21,21),PSIO(21,21),TT(21,21),
     & PSI(21,21),XI(21,21),XIO(21,21),BCON1(21),Tmr(21),ANU(1,21)
     & ,A1(21),B1(21),C1(21),D1(21),RERT(21,21),TO(21,21),T(21,21)
     & ,FANG(21),ANUT(21,21),TOO(21,21)

      OPEN(14,FILE='TEMP.DAT',STATUS='OLD')
      OPEN(4,FILE='fluid.DAT',STATUS='OLD')

      OPEN(16,FILE='TEMP.OUT',STATUS='NEW')
      OPEN(17,FILE='TPLOT.OUT',STATUS='NEW')
      OPEN(19,FILE='NUPLOT.OUT',STATUS='NEW')
C
C     NN : no. of grids in the radial direction
C     MM : no. of grids in the PHI -  direction
C
C___________________________________________________________________


C
C*****              { Convergence Parameters }
C___________________________________________________________________

      ALDTc=30.0
      ALDT=30.0
      MM=20
      NN=20
      DELr=1.0/NN
      DELph=3.141592654/MM


C     -----------------------------------------------------------

C     INITIAL FEILD

C     -----------------------------------------------------------

      print*,'REE='
      Read*,REE
C     Ro is the curvature ratio.
C     W, PSI, XI are the axial velocity, stream function and vortisity.
c=======
      print*,'Ro='
      Read*,Ro
c=======
      print*,'Pr='
      Read*,pr
c=======
      DO 707,K=1,MM+1
      DO 706,J=1,NN+1

      READ(4,*)W(J,K),XI(J,K),PSI(J,K)
c     READ(4,*)Wm

 706  CONTINUE
 707  CONTINUE

      IRUN=2
      IF(IRUN.EQ.2) THEN
```

```
      DO 702,J=1,NN+1
      READ(14,*)TO(J,K)
702   CONTINUE
      ELSE
      DO 604,K=1,MM+1
      DO 604,J=1,NN+1
      r=1.0D0-(J-1)*DELr
      TO(J,K)=1.0D0
604   CONTINUE
      ENDIF

C
C*****                  { Flow Considerations }
C



      IJK=1
C
999   DO 1000,J=1,NN+1
      DO 1000,K=1,MM+1
1000  TOO(J,K)=T(J,K)


C--------------------------------------------------------------------------
C     START OF T ( i+1/2 ) AT THE VERTICAL CENTER - LINE
C--------------------------------------------------------------------------

      K=MM/2+1
      PHI=0.0D0
      DO 1,J=2,NN
      r=1.0D0-(J-1)*DELr
      RR=Ro

      AT=1.0/r-Pr/r/(PSI(J,K+1)-PSI(J,K-1))/2.0/DELph
      BT=Pr/r/(PSI(J-1,K)-PSI(J+1,K))/2.0/DELr

      QT=-W(J,K)*TO(j,k)/TO(NN+1,MM/2+1)

      X1T=AT/2.0/DELr+1.0/DELr**2

      X2T=1.0/r**2/DELph**2-BT/2.0/DELph

      X4T=BT/(2.0*DELph)+1.0/(r*DELph)**2

      X5T=1.0/DELr**2-AT/2.0/DELr

      Xr1T=-2.0/DELr**2

      Xr2T=-2.0/r**2/DELph**2

      Xt1T=-2.0/r**2/DELph**2

      Xt2T=-2.0/DELr**2


      C1(J)=X5T
      A1(J)=X1T
```

```
      B1(J)=Xr1T

      D1(J)=QT-X2T*TO(J,K-1)-Xr2T*TO(J,K)-X4T*TO(J,K+1)
 1    CONTINUE


      DO 2,J=2,NN

      BCON=B1(NN/2+1)


      IF(J.LT.10) ALDTC=ALDTC*1.00

      B1(J)=B1(J)+BCON*ALDTc
      D1(J)=D1(J)+BCON*ALDTc*TO(J,K)
 2    CONTINUE

C     B C AT THE WALL
      A1(1)=0.0D0
      B1(1)=1.0D0
      C1(1)=0.0D0
      D1(1)=0.0D0

C     B C AT THE CENTER
      A1(NN+1)=-1.0D0
      B1(NN+1)=1.0D0
      C1(NN+1)=0.0D0
      D1(NN+1)=0.5D0*(TO(NN,K)-TO(NN+1,K))

      CALL DGTSL(NN+1,A1,B1,C1,D1,IFAIL)


      TO(NN+1,K)=D1(NN+1)

C     ____________________________________________________________

C     START OF T ( i+1/2 ) IN THE RADIAL DIRECTION

C     ____________________________________________________________

      DO 4,K=2,MM
      PHI=-3.141592654/2.0+(K-1)*DELph
      DO 5,J=2,NN
      r=1.0D0-(J-1)*DELr
      RR=Ro


      AT=1.0/r-Pr/r/(PSI(J,K+1)-PSI(J,K-1))/2.0/DELph
      BT=Pr/r/(PSI(J-1,K)-PSI(J+1,K))/2.0/DELr

      QT=-W(J,K)*TO(j,k)/TO(NN+1,MM/2+1)

      X1T=AT/2.0/DELr+1.0/DELr**2

      X2T=1.0/r**2/DELph**2-BT/2.0/DELph

      X4T=BT/(2.0*DELph)+1.0/(r*DELph)**2

      X5T=1.0/DELr**2-AT/2.0/DELr
```

```
      Xr1T=-2.0/DELr**2

      Xr2T=-2.0/r**2/DELph**2

      Xt1T=-2.0/r**2/DELph**2

      Xt2T=-2.0/DELr**2

      A1(J)=X1T
      B1(J)=Xr1T
      C1(J)=X5T
      D1(J)=QT-X2T*TO(J,K-1)-Xr2T*TO(J,K)-X4T*TO(J,K+1)
 5    CONTINUE


      DO 6,J=2,NN


      BCON=B1(NN/2+1)

      IF(J.LT.10) ALDT=ALDT*1.00

      B1(J)=B1(J)+BCON*ALDT
      D1(J)=D1(J)+BCON*ALDT*TO(J,K)
 6    CONTINUE

C     B C AT THE WALL
      A1(1)=0.0D0
      B1(1)=1.0D0
      C1(1)=0.0D0
      D1(1)=0.0D0

C     B C AT THE CENTER
      A1(NN+1)=0.0D0
      B1(NN+1)=1.0D0
      C1(NN+1)=0.0D0
      D1(NN+1)=TO(NN+1,MM/2+1)

      CALL DGTSL(NN+1,A1,B1,C1,D1,IFAIL)

      DO 7,J=1,NN+1
      T(J,K)=D1(J)
 7    CONTINUE

C-------------- UP DATING T IN EVERY r DIRECTION ---------

      DO 1001,J=1,NN+1
 1001 TO(J,K)=T(J,K)

C-----------------------------------------------------------

 4    CONTINUE

C     ----------------------------------------------------------

C     AT THE HORIZONTAL CENTER - LINE ( LHS ) AND ( RHS )
```

```
      DO 53,J=2,NN
      T(J,1)=(4.0D0*T(J,2)-T(J,3))/3.0D0
      T(J,MM+1)=(4.0D0*T(J,MM)-T(J,MM-1))/3.0D0
      T(NN+1,1)=T(NN+1,MM/2+1)
      T(NN+1,MM+1)=T(NN+1,MM/2+1)
 53   CONTINUE

C     ------------------------------------------------------------------
C     BOX A WHICH STORS THE NEW SOLUTION IN THE OLD STORS
C     ******************************************************************
      DO 104,K=2,MM
      DO 104,J=1,NN+1
      TO(J,K)=T(J,K)
 104  CONTINUE
C     *****

C     ------------------------------------------------------------------
C              START OF T ( i+1 ) IN PHI - DIRECTION
C     ------------------------------------------------------------------

      DO 16,J=2,NN
      DO 14,K=2,MM
      r=1.0D0-(J-1)*DELr
      PHI=-3.141592654/2.0+(K-1)*DELph

      RR=Ro

      AT=1.0/r-Pr/r/(PSI(J,K+1)-PSI(J,K-1))/2.0/DELph
      BT=Pr/r/(PSI(J-1,K)-PSI(J+1,K))/2.0/DELr

      QT=-W(J,K)*TO(j,k)/TO(NN+1,MM/2+1)

      X1T=AT/2.0/DELr+1.0/DELr**2

      X2T=1.0/r**2/DELph**2-BT/2.0/DELph

      X4T=BT/(2.0*DELph)+1.0/(r*DELph)**2

      X5T=1.0/DELr**2-AT/2.0/DELr

      Xr1T=-2.0/DELr**2

      Xr2T=-2.0/r**2/DELph**2

      Xt1T=-2.0/r**2/DELph**2

      Xt2T=-2.0/DELr**2


      A1(K)=X2T
      C1(K)=X4T
      B1(K)=Xt1T
```

```
        D1(K)=QT-X1T*TO(J-1,K)-Xt2T*TO(J,K)-X5T*TO(J+1,K)

 14     CONTINUE


        DO 18,K=2,MM

        BCON=B1(MM/2+1)

        IF(J.LT.10) ALDT=ALDT*1.00

        B1(K)=B1(K)+BCON*ALDT
        D1(K)=D1(K)+BCON*ALDT*TO(J,K)
 18     CONTINUE

C       B C AT THE WALL
        A1(1)=0.0D0
        B1(1)=1.0D0
        C1(1)=-1.0D0
        D1(1)=1.0D0/3.0D0*(TO(J,2)-TO(J,3))

C       B C AT THE CENTER
        A1(MM+1)=-1.0D0
        B1(MM+1)=1.0D0
        C1(MM+1)=0.0D0
        D1(MM+1)=1.0D0/3.0D0*(TO(J,MM)-TO(J,MM-1))

        CALL DGTSL(MM+1,A1,B1,C1,D1,IFAIL)

        DO 19,K=1,MM+1
        T(J,K)=D1(K)
 19     CONTINUE

C----------------------- UP DATING T IN EVERY PHI DIRECTION ---------

        DO 347,K=1,MM+1
        TO(J,K)=T(J,K)
 347    CONTINUE

C----------------------------------------------------------------------
 16     CONTINUE

C---------------------------------
CC      WRITE(17,*)ijk
        DO 906,K=2,MM
        DO 906, J=2,NN
        RERT(J,K)=ABS((T(J,K)-TOO(J,K))/T(J,K))
CC      WRITE(17,*)RERT(J,K)
 906    CONTINUE
C---------------------------------

        ermax=0.0
        DO 103 J=2,20
```

```
          DO 103 K=2,20
          IF(Rert(j,k).lt.Ermax) go to 103
          Ermax=RerT(j,k)
103       continue
c         write(17,*)'Ermax=',Ermax
          if(Ermax.lt.1.0e-5) go to 888

          IF(RERT(2,2).LT.1.0E-6.AND.RERT(5,5).LT.1.0E-6.AND.
     &   RERT(15,15).LT.1.0E-6.AND.RERT(10,18).LT.1.0E-6.AND.
     &    RERT(10,10).LT.1.0E-6.AND.RERT(7,3).LT.1.0E-6) THEN
          GOTO 888

          ELSE
C         BOX A WHICH STORS THE NEW SOLUTION IN THE OLD STORS

C         ******************************************************************

          DO 107,J=2,NN
          DO 106,K=1,MM+1
          TO(J,K)=T(J,K)
  106     CONTINUE
  107     CONTINUE

  997     CONTINUE
          IJK=IJK+1
          IF(IJK.GT.500) GOTO 888
          GOTO 999
          ENDIF

C         ******************************************************************



cc        WRITE(*,*)ijk
c 888     WRITE(17,*)'RELATIVE ERROR IN TEMP.'
 888      DO 807,K=1,MM+1
          DO 806,J=1,NN+1
          WRITE(16,*)TO(J,K)
c         WRITE(17,*)RERT(J,K)


  806     CONTINUE
          WRITE(16,*)'                                                  '
c         WRITE(17,*)'                                                  '
  807     CONTINUE
c         WRITE(17,*)'                                                  '

cc
CC
CC
CC   ********** CALCULATION OF THE BULK TEMPRATURE **********
CC
CC
CC
          DO 961 J= 1,21
CCCC      r=1.0-(j-1)*DELr
           SUM1 = 0.0
          DO 62 I=2,20,2
          r=1.0-(I-1)*DELr
```

```
         SUM1 = SUM1 +4.0*W(I,J)*T(I,J)*r
  62    CONTINUE
         SUM2 = 0.0
        DO 403 I= 3,19,2
        r=1.0-(I-1)*DELr
         SUM2 = SUM2 + 2.0*W(I,J)*T(I,J)*r
  403   CONTINUE
  961    FANG(J) = (DELr/3.0)*(SUM1+SUM2)
CC
     SUM1 = 0.0
     DO 404 J=2,20,2
         SUM1 = SUM1 + 4.0 * FANG(J)
  404   CONTINUE
     SUM2 = 0.0
     DO 405 J=3,19,2
405  SUM2 = SUM2 + 2.0 * FANG(J)
CC
     Tm=(4.0/(REE*3.141592654)) * (DELph/3.0) * (FANG(1) + SUM1+SUM2+
    &   FAN
    *         G(21))

        WRITE(17,*) ' Pr=',Pr,'  ERmax=',ermax
        WRITE(17,*) 'Ro=',Ro,' Re=',REE
c------------------   DT calculation ---------------

        Tmax=0.0
        do 102 j=1,21
        do 102 k=1,21
        if(t(j,k).lt.Tmax) go to 102
        Tmax=T(j,k)
102     continue
        write(17,*)'DT=',Tmax/10.0
        WRITE(17,*)'IJK=',IJK
CC      ----------------------------------
cc      CALCULATING LOCAL NU
C
        DO 905,K=1,MM+1
        ANU(1,K)=-2.0/Tm*(3.0*T(1,k)-4.0*T(2,K)+T(3,K))/2.0/DELr
  905   CONTINUE
C       ----------------------------------
CC      CALCULATING AVERAGE NU AT THE WALL

        SUM=0.0
        DO 903,K=2,MM
        SUM=SUM+ANU(1,K)
  903   CONTINUE
        AMNU=DELph/(2.0*3.141592654)*(ANU(1,1)+ANU(1,MM+1)+2.0*SUM)
        WRITE(17,*)'AMNU=' ,AMNU
C=========================================================
        WRITE(19,*)MM+1
        DO 555,K=1,MM+1
        PHI=(-3.141592654/2.0+(K-1)*DELph)*180.0/3.141592654
        WRITE(19,*)PHI,',',ANU(1,K)
  555   CONTINUE

C       AT THE HORIZONTAL CENTER - LINE ( LHS )
        WRITE(17,*) 2*NN+1
        DO 551,J=1,NN
        WRITE(17,*)-(1.0D0-(J-1)*DELr),',', T(J,1)
  551   CONTINUE
```

```
      WRITE(16,*) '                                    '
C     AT THE HORIZONTAL CENTER - LINE ( RHS )
      WRITE(17,*) 0,',',T(NN+1,1)
      DO 552,J=NN,1,-1
      WRITE(17,*) 1.0D0-(J-1)*DELr,',',T(J,MM+1)
  552 CONTINUE
c

      NPLOT=2
      CALL CPLOT ( T,PGRAD,RO, DE, RE,Pr,IWORK,NPLOT)
      stop
      end
```

# خلاصة

في هذا البحث تم دراسه التدفق اللزج وانتقال الحراره في الملفات الحلزونيه بطريقه عدديه حيث دُرس تاثير خطوه الملف على تدفق المائع وانتقال الحراره . وقد افترض في الدراسه ان نصف قطر الملف اكبر بكثير من نصف قطر الانبوب الذى يكوّن الملف . والفرض الاخر يتعلق بالظرف الحدي الحراري حيث تم اعتبار درجه حراره الحائط ثابته ، اما ( Prandtl Number ) فيراوح ضمن المجال ( 0.05-40 ) بينما ( Dean Number ) فيراوح ضمن المجال ( 60-320 ) ونسبه انحناء الملف التي كانت الدراسه وفقا لها هي 100 .

وقد تم استخدام الطريقه العدديه المسماة (الاسلوب الضمني ذى الاتجاه المتغير) ( ADI ) من اجل حل مجالات التدفق والحراره . ولوحظ ان الحل العددى يكون مستقراً على نحو جيد عندما يتم توظيف معامل تقاربي في ال ( ADI ) .

وكنتيجه للدراسه تبين ان زاويه خطوه الملف لغايه $30^\circ$ لها تاثير متواضع على انتقال الحراره بطريقه الحمل ، ومع ذلك فقد لوحظ ان زوايا الخطوه لغايه $45^\circ$ تعمل على تقليل القيمه المتوسطه ل ( Nusselt Number ) بمقدار 20% في حاله القيم المتوسطه والعاليه ل ( Prandtl Number ) ، بينما هذا التاثير يصل في حاله القيم المتدنيه ل ( Prandtl Number ) الى ما نسبته 10% .